Mathematical Biology



Dynamics of task allocation in social insect colonies: scaling effects of colony size versus work activities

Tao Feng^{1,2} · Daniel Charbonneau³ · Zhipeng Qiu¹ · Yun Kang²

Received: 17 April 2020 / Revised: 26 October 2020 / Accepted: 28 February 2021 /

Published online: 29 March 2021

© The Author(s), under exclusive licence to Springer-Verlag GmbH Germany, part of Springer Nature 2021

Abstract

The mechanisms through which work is organized are central to understanding how complex systems function. Previous studies suggest that task organization can emerge via nonlinear dynamical processes wherein individuals interact and modify their behavior through simple rules. However, there is very limited theory about how those processes are shaped by behavioral variation within social groups. In this work, we propose an adaptive modeling framework on task allocation by incorporating variation both in task performance and task-related metabolic rates. We study the scaling effects of colony size on the resting probability as well as task allocation. We also numerically explore the effects of stochastic noise on task allocation in social insect colonies. Our theoretical and numerical results show that: (a) changes in colony size can regulate the probability of colony resting and the allocation of tasks, and the direction of regulation depends on the nonlinear metabolic scaling effects of tasks; (b) increased response thresholds may cause colonies to rest in varied patterns such as periodicity. In this case, we observed an interesting bubble phenomenon in the task allocation of social insect colonies for the first time; (c) stochastic noise can cause work activities and task demand to fluctuate within a range, where the amplitude of the fluctuation is positively correlated with the intensity of noise.

Keywords Social insects \cdot Task allocation \cdot Colony size \cdot Adaptive stimulus \cdot Resting \cdot Metabolic rate \cdot Environmental noises

Mathematics Subject Classification 34D23 · 92B05 · 34F05

This research is funded by the NSF-DMS (Award Number 1716802); the NSF-IOS/DMS (Award Number 1558127); DARPA-SBIR 2016.2 SB162-005; and the James S. McDonnell Foundation 21st Century Science Initiative in Studying Complex Systems Scholar Award (UHC Scholar Award 220020472). T. Feng was partially funded by the Outstanding Chinese and Foreign Youth Exchange Program of China Association of Science and Technology; and the Scholarship Foundation of China Scholarship Council (Award Number 201806840120). Z. Qiu was funded by the National Natural Science Foundation of China (Award Number 12071217, 11671206).

Extended author information available on the last page of the article



42 Page 2 of 53 T. Feng et al.

1 Introduction

Social insect colonies are often considered to be highly efficient complex systems that dominate most terrestrial ecosystems across the planet (Hölldobler and Wilson 2009; Wilson 1971). The success of social insect colonies is often attributed to their sophisticated and complex mechanisms for organizing work leading to division of labor and efficient task allocation in dynamic environments, and as the colony grows (Gordon 1996; Robinson et al. 2009). Colony size plays an essential role in the development of social insect colonies, and profoundly affects many aspects of colony function, such as foraging (Beckers et al. 1989; Mailleux et al. 2003; Thomas and Framenau 2005); collective decision-making strategies (Franks et al. 2006; Ruel et al. 2012); workload distributions (Dornhaus et al. 2008) and social organization (Bourke 1999). Previous studies have shown that colony size plays a vital role in task allocation (ants (Holbrook et al. 2013, 2011; Tschinkel 1993); bees (Bourke 1999); wasps (Jeanne 2003) and termites (Hou et al. 2010)). There is significant empirical work looking at the internal relationship between colony size and task organization (Fewell and Harrison 2016; Gordon 1996; Fjerdingstad and Crozier 2006; Jeanson et al. 2007; Dornhaus et al. 2012), however, theoretical work remains limited. At the same time, the mechanisms through which colony size influences task allocation, are not wellunderstood. We know that metabolic rates do not scale linearly with body size in most living organisms (i.e., metabolic rates are proportionately lower in larger organisms (Kleiber 1932, 1947; Glazier 2010)). The same pattern has been shown to occur in social insect colonies (often conceived of as 'superorganisms') where per-capita metabolic rates decrease with colony size (Fewell and Harrison 2016; Waters 2014; Shik 2010; Waters et al. 2010). Therefore, it is essential to include metabolic rates of workers performing varied tasks when studying the organization of work.

Inactivity has long been known to be one of the most common behaviors observed in social insect colonies (Hölldobler and Wilson 1990). Indeed, at any given moment, there are typically 40–70% of workers in a colony that are inactive (honey bees (Lindauer 1952; Moore et al. 1998; Muscedere et al. 2009); bumblebees (Jandt et al. 2012); wasps (Gadagkar and Joshi 1984); termites (Maistrello and Sbrenna 1999) and ants (Herbers and Cunningham 1983; Herbers 1983; Cole 1986; Corbara et al. 1989; Retana and Cerdá 1990; Dornhaus 2008; Charbonneau et al. 2015)). Additionally, some individuals appear to spend a disproportionate amount of time inactive, effectively specializing on inactivity (Herbers and Cunningham 1983; Fresneau 1984; Cole 1986; Retana and Cerdá 1990; Retana and Cerda 1991). Inactivity levels in the field have been shown to be comparable to those observed in lab colonies, suggesting that these high levels of inactivity are not simply an artifact of simplified conditions in the lab (Charbonneau et al. 2015).

Although inactivity is widespread in social insect colonies, its role in colony function is not well understood and rarely taken into account in the study of task allocation, which may cause potential bias (Charbonneau and Dornhaus 2015b). We do not currently know what shape of 'inactivity demand' (i.e., the function describing the distribution of inactivity in a colony) might resemble in colonies. Individuals likely have a base requirement for rest which they need to attain to remain functional. There is evidence of decreased performance in sleep-deprived bees (Klein et al. 2010). Fur-



thermore, the base amount of inactivity needed is probably a function of other factors, such as worker age (D. Charbonneau, unpublished results, also see Muscedere et al. 2009 for inactivity due to worker immaturity). However, there is most like an additional amount of inactivity that results from insufficient work (see Charbonneau and Dornhaus 2015a for conceptual framework). Thus, we should expect inactivity demand to result from both a constant function (base need for rest) as well as an increasing function (dependent on a combination of available work/colony needs and available workforce). Our modeling work incorporates both.

Mathematical models have been successfully applied to many aspects of social insect behavioral dynamics (Chen et al. 2020; Guo et al. 2020; Messan et al. 2018, 2020), such as genetic variability (Kang and Fewell 2015; Myerscough and Oldroyd 2004); foraging activities (Ramsch et al. 2012; Udiani et al. 2015); evolutionary dynamics (Kang et al. 2015) and task allocation (Bonabeau et al. 1997; Cornejo et al. 2014; Rodriguez et al. 2018; Rodriguez-Rodriguez and Kang 2016). Most of these models are useful and focusing on simulations to explore the dynamics of social insect colonies. They intuitively show the physical characteristics of social insect colonies and provide scientists with an inexhaustible motivation for a deeper understanding of social insect colonies. Differential equations have proven to be highly effective in revealing the principles and laws behind different representations. In recent years, differential equations have been gradually employed by scholars to study the dynamical processes of social insect colonies (see some interesting topics that have been explored in Kang and Theraulaz 2016, Sumpter and Pratt 2003). In this study, we would use ordinary differential equations (ODEs) and stochastic differential equations (SDEs) as our modeling tools.

Social insects live in a dynamic environment and are inevitably affected by random fluctuations (e.g., stochastic noises). Studies have shown that random fluctuations can potentially positively or negatively affect the dynamical outcomes of social insect colonies (Cammaerts and Cammaerts 2018; Dussutour et al. 2009; Feinerman and Korman 2017). Due to the ever-changing environment, there are many types of stochastic noises (e.g., white noise (DeLillo 1999); telegraph noise (Ranjan et al. 2016)). Currently, various methods have been developed to characterize different types of environmental noises such as Brownian motion (Saffman and Delbrück 1975) and also Markov switch (Slatkin 1978). In recent years, stochastic models based on random fluctuations have been successfully applied in many scientific fields, such as epidemic dynamics (Allen and Lahodny 2012; Britton 2010; Cai et al. 2020, 2017; Gray et al. 2011) and population dynamics (Benaïm and Schreiber 2019; Hening et al. 2018; Ovaskainen and Meerson 2010; Wu and Xu 2009). However, as far as we know, many current modeling frameworks for social insect colonies are mostly based on deterministic models (Banks et al. 2017; Kang and Theraulaz 2016; Magal et al. 2019; Sumpter and Pratt 2003) with few studies that have used stochastic models (but see Arcuri and Lanchier 2017; Dussutour et al. 2009). Thus, we will start with ODEs and then add random fluctuations through SDEs to study the impacts of random fluctuations.

This paper proposes a theoretical framework at the colony level to study task allocation dynamics of social insect colonies. Internal factors (e.g., the various threshold for different tasks) and external factors (e.g., task stimuli from the environment) that may



42 Page 4 of 53 T. Feng et al.

affect task allocation are incorporated into the proposed theoretical framework. The theoretical output is expected to address the following issues: (i) how does metabolic scaling affect task allocation and resting probability of social insect colonies, as colony size increases? (ii) how does colony size affect working activity in different scenarios of working versus resting? (iii) how does random fluctuation affect working activity and task demand of social insect colonies?

The rest of the paper is organized as follows: Sect. 2 presents the model derivation of task allocation. Section 3 begins by laying out the mathematical analysis of the theoretical framework (i.e., the invariant set of positive solution and the existence of equilibrium), and addresses the scaling effects of colony size on resting probability and task allocation. Section 4 is concerned with the application of the theoretical framework: working activities versus resting models in four different scenarios. The global dynamics of the proposed models are studied theoretically, and the effects of factors (including colony size and metabolic scaling) on work activities are analyzed biologically. Section 5 assumes that task demand is subject to random fluctuations, and studies the effects of random fluctuations on task demand and work activities. Section 6 presents a summary of the results and discusses their related biological significance.

2 Model derivation of task allocation

Let $N \ge 1$ be the total population size of the colony; $m \ge 1$ be the number of tasks in a social insect colony; $D = [D_0, D_1, D_2, \cdots, D_m]$ be the task demand where D_0 is the demand of inactive (i.e., resting) and D_i , i = 1, ..., m is the demand of the specific task $i; X = [x_0, x_1, x_2, \cdots, x_m]$ be the task allocation for m tasks where $x_i, 1 \le i \le m$ is the ratio of workers performing task i and x_0 is the portion of workers being inactive (i.e., resting). Therefore, for each task i, there are Nx_i workers performing the task i. In the case that N = 1 (e.g., when the single queen establishes her own colony), $x_i \in [0, 1]$ could be considered as the allocation of energy/time to perform task i when $0 \le i \le m$ or the resting time i = 0.

Let θ_i be an average response threshold for task i for a colony, and we can define $\frac{D_i}{\theta_i}$ as the relative stimulus of task i. Then, the larger demand D_i and/or the smaller average response threshold θ_i gives the larger relative stimulus for task group i. Therefore, we

can define $f_i = \frac{\frac{D_i x_i}{\theta_i}}{\sum_{k=0}^{m} \frac{D_k x_k}{\theta_k}}$ as the recruitment ability of task i, and the dynamics of

task *i* allocation, i.e., $\frac{dx_i}{dt}$, can be modeled as follows:

$$\frac{dx_i}{dt} = \sum_{k=0, k \neq i}^{m} f_i x_k$$

workers performing other tasks switching to task i

$$- \sum_{k=0, k \neq i}^{m} f_k x_i$$

workers performing task i switching to other tasks



$$= f_i(1 - x_i) - x_i(1 - f_i) = f_i - x_i = x_i \left[\frac{\frac{D_i}{\theta_i}}{\sum_{k=0}^{m} \frac{D_k x_k}{\theta_k}} - 1 \right].$$

The demand of task i of the colony, i.e., D_i , is determined by the following two factors:

- The demand input $\gamma_i N^{\delta_i}$ is an increasing nonlinear function of the colony size N, where γ_i represents the increase in demand intensity per unit time for task i and δ_i denotes the nonlinear metabolic scaling of task i from the colony size N. The formulation of this demand input follows the metabolic scaling effects in ecology (Chown et al. 2007). Much literature reported that the values of δ_i for social insect colonies are less than one (Waters et al. 2010), but for some species they could also be above one depending on caste and the related tasks (Shik 2010).
- The depletion of demand $\alpha_i N x_i D_i$ is an increasing function of the demand D_i and the size of task group $N x_i$, where α_i denotes the average performance efficiency of task group i. This modeling approach is adopted from Kang and Theraulaz 2016 (but also see the work of Theraulaz et al. 1998), which gives the dynamics of the demand for task i that could be modeled by follows:

$$D_i' = \gamma_i N^{\delta_i} - \alpha_i N x_i D_i = \gamma_i N^{\delta_i} \left[1 - \frac{\alpha_i x_i N^{1 - \delta_i}}{\gamma_i} D_i \right] = \gamma_i N^{\delta_i} \left[1 - \frac{x_i D_i}{\theta_i \hat{D}_i} \right].$$

We assume that the relative stimulus of inactivity/resting could be either a constant, e.g., $\frac{D_0}{\theta_0} = \Phi N^{\delta_0}$, or an increasing function of working effort $1 - x_0$ such as $\frac{D_0}{\theta_0} = w N^{\delta_0} (1 - x_0)$.

The discussion above provides a general dynamical compartmental model of task allocation on the colony level that can be represented as the following set of nonlinear compartment model:

$$x_{i}' = x_{i} \left[\frac{\frac{D_{i}}{\theta_{i}}}{\sum_{k=0}^{m} \frac{D_{k}x_{k}}{\theta_{k}}} - 1 \right], i \geq 0,$$

$$D_{i}' = \gamma_{i} N^{\delta_{i}} \left[1 - \frac{x_{i}D_{i}}{\theta_{i}\hat{D}_{i}} \right], i \geq 1,$$

$$(1)$$

where $\frac{D_0}{\theta_0} = \Phi N^{\delta_0}$ or $\frac{D_0}{\theta_0} = w N^{\delta_0} (1 - x_0)$; and $\hat{D}_i = \frac{\gamma_i N^{\delta_i - 1}}{\alpha_i \theta_i}$. The proposed general Model (1) incorporates both variation in task performance among workers and individual worker flexibility. The decision of an individual worker performing a task depends on both the internal factors (e.g., the varied thresholds for different tasks) and the external factors (e.g., task needs from the environment). Thus, the dynamical outcomes of Model (1) are expected to predict how colonies allocate workers in relation to the need for each task and adjust the allocation in response to environmental changes as well as its colony size N. As a note, we would like to point out that Model (1) can also model how the solitary foundress queen allocates her energy and time



42 Page 6 of 53 T. Feng et al.

for different tasks when N = 1. And if m = 1, Model (1) models how social insect colonies decide on working x_1 or resting x_0 depending on the work demand D_1 and the environmental changes.

Social insect colonies live in the ever-changing environment that is subject to random fluctuations (e.g., see Cammaerts and Cammaerts 2018; Dussutour et al. 2009; Feinerman and Korman 2017), especially the demand of each task D_i . By using standard techniques (Evans et al. 2013; Hening et al. 2018), for any initial demand $D_i(0) = D_0^i$ and time step $0 \le \Delta t \ll 1$, the task demand $D_i(t)$ can be described by a Markov process with conditional mean

$$\mathbb{E}[D_i(t + \Delta t) - D_i(t)|D_i(t) = D_0^i] \approx \gamma_i N^{\delta_i} \left[1 - \frac{x_i D_i}{\theta_i \hat{D}_i}\right] \Delta t$$

and conditional covariance

$$Cov[D_i(t + \Delta t) - D_i(t)|D_i(t) = D_0^i] \approx \sigma_{ij}D_iD_j\Delta t$$

for some covariance matrix $\Sigma = (\sigma_{ij})$. More formally, it is natural to include random fluctuations into the demand dynamics through the following SDEs:

$$dx_{i} = x_{i} \left[\frac{\frac{D_{i}}{\theta_{i}}}{\sum_{k=0}^{m} \frac{D_{k}x_{k}}{\theta_{k}}} - 1 \right] dt, i \geq 0,$$

$$dD_{i} = \gamma_{i} N^{\delta_{i}} \left[1 - \frac{x_{i}D_{i}}{\theta_{i}\hat{D}_{i}} \right] dt + \sigma_{i}D_{i}(t)dB_{i}(t), i \geq 1,$$

$$(2)$$

where $B_i(t)$ is a standard one-dimensional independent Brownian motion defined on the complete probability space $(\Omega, \mathcal{F}, \mathbb{P})$, and σ_i^2 is the intensity of $B_i(t)$. The dynamics x_i is the ratio thus it is confined in [0,1), and the sum of all x_i should be 1. It is not reasonable to include environmental stochasticity by using the approach of modeling environmental stochasticity in D_i . The dynamics of x_i is affected by D_i whose dynamics include environmental stochasticity, thus x_i in fact has demographic stochasticity from its demand dynamics D_i . We assume that the parameters θ_i , γ_i , δ_i are constant but it would be realistic to include stochasticity in those parameter values.

In the next section, we will provide theoretical results of our ODE Model (1) predictions and the related biological implications. And the SDE Model (2) will be explored in Sect. 5.

3 Mathematical analysis

Notice that $\sum_{k=0}^{m} x_k' = 0$ in Model (1), therefore, $S = \{\sum_{i=0}^{m} x_i = 1 : 0 \le x_i \le 1\}$ is the invariant set. The state space of Model (1) could be defined as $\Omega = S \times \mathbb{R}_+^m$.



Let $\hat{D}_i = \frac{\gamma_i N^{\delta_i - 1}}{\alpha_i \theta_i}$ be the efficient demand for task i, and define $\hat{D} = \sum_{k=1}^m \hat{D}_k$ as the total efficient demand for all tasks in the colony.

Theorem 1 (Dynamical Properties) Assume that all parameters are strictly positive and $\sum_{i=0}^{m} x_i(0) = 1$ with $x_i(0) > 0$ for all i = 0, ..., m. Then the model (1) is positively invariant and bounded in Ω with

$$\liminf_{t\to\infty} D_i(t) \ge \frac{\gamma_i N^{\delta_i-1}}{\alpha_i} = \theta_i \hat{D}_i \text{ for any } i = 1, ..., m.$$

Let $\frac{D_0}{\theta_0} = \Phi N^{\delta_0}$, then we have

1. If $\Phi N^{\delta_0} < \hat{D}$, Model (1) has a unique equilibrium (X^*, D^*) with

$$x_0^* = 0$$
, $x_i^* = \frac{\hat{D}_i}{\hat{D}}$ and $D_i^* = \hat{D}\theta_i$, for all $1 \le i \le m$.

2. If $\Phi N^{\delta_0} > \hat{D}$, Model (1) has a unique interior equilibrium (\hat{X}^*, \hat{D}^*) with

$$\hat{x}_0^* = 1 - \frac{\hat{D}}{\Phi N^{\delta_0}}, \ \hat{x}_i^* = \frac{\hat{D}_i}{\Phi N^{\delta_0}} \ and \ \hat{D}_i^* = \Phi \theta_i N^{\delta_0}.$$

Let $\frac{D_0}{\theta_0} = wN^{\delta_0}(1-x_0)$, then we have

1. If $wN^{\delta_0} < \hat{D}$, Model (1) has a unique equilibrium (X^*, D^*) with

$$x_0^* = 0, \ x_i^* = \frac{\hat{D}_i}{\hat{D}} \ and \ D_i^* = \hat{D}\theta_i.$$

2. If $wN^{\delta_0} > \hat{D}$, Model (1) has a unique interior equilibrium (\hat{X}^*, \hat{D}^*) with

$$\hat{x}_0^* = 1 - \sqrt{\frac{\hat{D}}{wN^{\delta_0}}}, \ \hat{x}_i^* = \frac{\hat{D}_i}{\sqrt{\hat{D}wN^{\delta_0}}} \ and \ \hat{D}_i^* = \theta_i \sqrt{\hat{D}wN^{\delta_0}}.$$

Moreover, if there exists an i such that $wN^{\delta_0} < \hat{D}_i$ for $\frac{D_0}{\theta_0} = wN^{\delta_0}(1-x_0)$ or $\frac{D_0}{\theta_0} = \Phi N^{\delta_0} < \hat{D}_i$ holds, we have

$$\lim_{t\to\infty}x_0(t)=0.$$

Biological implications Theorem 1 suggests that our model (1) is well defined biologically. Numerical simulations suggest that for all initial conditions in the interior of S, i.e., $\{\sum_{i=0}^m x_i(0) = 1 : 0 < x_i(0) \le 1\}$, the unique equilibrium (X^*, D^*) is always globally stable when the total efficient demand for all tasks is large (e.g., $\Phi N^{\delta_0} < \hat{D}$ or $wN^{\delta_0} < \hat{D}$). Otherwise, the unique interior equilibrium (\hat{X}^*, \hat{D}^*) is always globally stable. More specifically, our results have the following implications:



42 Page 8 of 53 T. Feng et al.

1. If there is a task whose *efficient demand* (i.e., \hat{D}_i , $1 \le i \le m$) is larger than the physiological resting demand ΦN^{δ_0} (or wN^{δ_0}), the colony has no allocation to resting due to the demand requirement.

- 2. If there is no allocation to resting due to high task demand, the specific allocation for task *i* is determined by the ratio of *the efficient demand for task i* to *the total efficient demand for all tasks* in the colony, i.e., $x_i^* = \frac{\hat{D}_i}{\hat{D}}$.
- 3. If the physiological resting demand ΦN^{δ_0} (or wN^{δ_0}) is larger than the total efficient demand for all tasks, the allocation for task i is determined by the ratio of the efficient demand for task i to the physiological resting demand in the colony, i.e., $\hat{x}_i^* = \frac{\hat{D}_i}{\Phi N^{\delta_0}}$ (for the case of ΦN^{δ_0}) or $\hat{x}_i^* = \frac{\hat{D}_i}{\sqrt{\hat{D}wN^{\delta_0}}}$ (for the case of wN^{δ_0}).

3.1 Scaling effects of the colony size N on the resting probability

Define
$$G(N) = \frac{\hat{D}}{N^{\delta_0}} = \sum_{k=1}^m \frac{\gamma_k N^{\delta_k - \delta_0 - 1}}{\alpha_k \theta_k}$$
, then
$$\frac{dG(N)}{dN} = \sum_{k=1}^m \frac{\gamma_k (\delta_k - \delta_0 - 1) N^{\delta_k - \delta_0 - 2}}{\alpha_k \theta_k}.$$
 (3)

According to Theorem 1, we know that the value of Φ (or w) and G(N) determines whether the colony will rest, i.e.,

$$\frac{D_0}{\theta_0} = \Phi N^{\delta_0} < \hat{D} \Leftrightarrow \Phi < G(N) \text{ and } wN^{\delta_0} < \hat{D} \Leftrightarrow w < G(N).$$

Note that δ_i represents the nonlinear metabolic scaling of task i from the colony size N, the Eq. (3) implies follows:

- 1. If the nonlinear metabolic scaling of all tasks is larger than the sum of the nonlinear metabolic scaling of resting and 1, i.e., $\delta_k > \delta_0 + 1$ for all $1 \le k \le m$, we have $\frac{dG(N)}{dN} > 0$, which implies that increasing the colony size N can increase the value of G(N), thus the inequality $\Phi < G(N)$ or w < G(N) is more likely to hold. Therefore, increasing the colony size N can decrease the probability of the colony resting.
- 2. If the nonlinear metabolic scaling of all tasks is smaller than the sum of the nonlinear metabolic scaling of resting and 1, i.e., $\delta_k < \delta_0 + 1$ for all $1 \le k \le m$, we have $\frac{dG(N)}{dN} < 0$, which implies that increasing the colony size N can decrease the value of G(N), thus the inequality $\Phi < G(N)$ or w < G(N) is not likely to hold. Therefore, increasing the colony size N can increase the probability of the colony resting.

If there are some tasks whose nonlinear metabolic scaling is larger than $\delta_0 + 1$ while some others is smaller than $\delta_0 + 1$, the situation becomes complicated. To further investigate the effects of the colony size, we focus on the two task cases m = 2, e.g., the inside colony task (i = 1) versus the outside colony task (i = 2). For simplicity,



we assume that $\delta_1 < \delta_0 + 1 < \delta_2$. Then we have

$$\begin{split} \frac{dG(N)}{dN} &= \frac{\gamma_{1}(\delta_{1} - \delta_{0} - 1)N^{\delta_{1} - \delta_{0} - 2}}{\alpha_{1}\theta_{1}} + \frac{\gamma_{2}(\delta_{2} - \delta_{0} - 1)N^{\delta_{2} - \delta_{0} - 2}}{\alpha_{2}\theta_{2}} \\ &= \frac{\gamma_{1}(\delta_{0} + 1 - \delta_{1})N^{\delta_{1} - \delta_{0} - 2}}{\alpha_{1}\theta_{1}} \left[-1 + \frac{\gamma_{2}\alpha_{1}\theta_{1}(\delta_{2} - \delta_{0} - 1)N^{\delta_{2} - \delta_{1}}}{\gamma_{1}\alpha_{2}\theta_{2}(\delta_{0} + 1 - \delta_{1})} \right], \end{split}$$
(4)

which implies that

$$\frac{dG(N)}{dN} > 0 \text{ if } N > \left(\frac{\gamma_1 \alpha_2 \theta_2 (\delta_0 + 1 - \delta_1)}{\gamma_2 \alpha_1 \theta_1 (\delta_2 - \delta_0 - 1)}\right)^{\frac{1}{\delta_2 - \delta_1}}$$

and

$$\frac{dG(N)}{dN} < 0 \text{ if } N < \left(\frac{\gamma_1 \alpha_2 \theta_2 (\delta_0 + 1 - \delta_1)}{\gamma_2 \alpha_1 \theta_1 (\delta_2 - \delta_0 - 1)}\right)^{\frac{1}{\delta_2 - \delta_1}}.$$

Take $N_c = \left(\frac{\gamma_1\alpha_2\theta_2(\delta_0+1-\delta_1)}{\gamma_2\alpha_1\theta_1(\delta_2-\delta_0-1)}\right)^{\frac{1}{\delta_2-\delta_1}}$ as the population threshold of a colony that determines whether a colony is mature or not. Based on the discussions above, we can conclude that if the colony size is less than the threshold, i.e., $N < N_c$ (e.g., immature colony), increasing the colony size N can increase the probability of the colony resting, while if $N > N_c$, increasing the colony size N can decrease the probability of the colony resting.

Biological Scenarios 3.11 Because of the physiological need for rest, or behavioral sleep in insects (Klein et al. 2003, 2010), all workers should need to spend a certain amount of time inactive. Thus, all workers should be expected to have more or less similar needs, and consequently have comparable levels of inactivity. We also know that workers can vary in activity levels over the course of the day (circadian rhythms Charbonneau and Dornhaus 2015b; Klein and Seeley 2011) and between seasons (Fellers 1989), as well as specific tasks that they perform, complex activity patterns can arise when these interact (Pol and de Casenave 2004). Our theoretical results support that when the nonlinear metabolic scaling for active tasks is large enough (i.e., larger than 1 + the nonlinear metabolic scaling of resting; or the energetic input of tasks increases with colony size), that larger colonies will have proportionally less inactive workers. This could be explained, for example, by increased difficultly in moving around in and accessing different tasks in larger colonies (Naug 2009), decreased efficiency in communicating task demand/stimulus (Beckers et al. 1989), the need to exploit exponentially larger foraging areas to meet the needs of larger colonies (Tschinkel et al. 1995), all of which would result in overall decreased per capita efficiency (i.e., greater overhead costs) in larger groups. Empirical data shows that larger colonies typically have less per capita inactive workers (Schmid-Hempel 1990), suggesting that large nonlinear metabolic scaling effects may be common in social insect colonies.



42 Page 10 of 53 T. Feng et al.

Alternatively, our theoretical results also suggest that when the nonlinear metabolic scaling of all tasks is smaller than the sum of the nonlinear metabolic scaling of resting and 1 (i.e., tasks become less energetically costly as colonies increase in size/more efficient), larger colonies may have proportionally more inactive ants. One potential explanation is that ants in larger colonies may have decreased locomotor activity (Waters et al. 2010), which would result in lower metabolic costs (though, potentially, decreased locomotor activity may result in less efficient communication and task performance, which would have the inverse effect). Meanwhile, because the metabolic rate of inactive ants can be significantly lower than active ants (Lighton et al. 1987), increases in the proportion of inactive ants in larger colonies will result in lower mass-specific metabolic rate. Another potential explanation is that larger colonies can sometimes have on average heavier workers (Tschinkel 1993; Blanchard et al. 2000; Robinson et al. 2009), though it is unclear that whether and how body size correlates to colony size in social insects (Dornhaus et al. 2012).

3.2 Scaling effects of the colony size N on the task allocation

We now focus on the effects of colony size on task allocation in situations where there are two task groups (i.e., m = 2, an inside nest task group and outside nest task group).

3.2.1 Resting demand is constant and smaller than task demand

According to Theorem 1, we know that if the relative stimulus of resting $\frac{D_0}{\theta_0} = \Phi N^{\delta_0}$ is smaller than the relative stimulus of working \hat{D} , i.e., $\frac{D_0}{\theta_0} = \Phi N^{\delta_0} < \hat{D}$ (or $wN^{\delta_0} < \hat{D}$ when the relative stimulus of resting is denoted by $\frac{D_0}{\theta_0} = wN^{\delta_0}(1-x_0)$), the colony works all the time with the following task allocation:

$$x_1^* = \frac{\hat{D}_1}{\hat{D}} = \frac{\frac{\gamma_1 N^{\delta_1 - 1}}{\alpha_1 \theta_1}}{\frac{\gamma_1 N^{\delta_1 - 1}}{\alpha_1 \theta_1} + \frac{\gamma_2 N^{\delta_2 - 1}}{\alpha_2 \theta_2}} = \frac{1}{1 + \frac{\gamma_2 \alpha_1 \theta_1 N^{\delta_2 - \delta_1}}{\gamma_1 \alpha_2 \theta_2}} \text{ and } x_2^* = 1 - x_1^*.$$

Therefore, we have

$$\frac{dx_1^*}{dN} = \frac{\gamma_1 \gamma_2 \alpha_1 \alpha_2 \theta_1 \theta_2 N^{\delta_2 - \delta_1 - 1}}{\left(\gamma_1 \alpha_2 \theta_2 + \gamma_2 \alpha_1 \theta_1 N^{\delta_2 - \delta_1}\right)^2} (\delta_1 - \delta_2) \text{ and } \frac{dx_2^*}{dN} = -\frac{dx_1^*}{dN}.$$
 (5)

The Eq. (5) indicates follows:

- 1. If the nonlinear metabolic scaling of the inside colony task δ_1 is the same as the outside colony task δ_2 , i.e., $\delta_2 = \delta_1$, the Eq. (5) implies that the colony size N has no effects on the task allocation.
- 2. If the nonlinear metabolic scaling of the inside colony task δ_1 is smaller than the outside colony task δ_2 , i.e., $\delta_2 > \delta_1$, the Eq. (5) implies that the colony size N has negative effects on the allocation of the inside colony task and positive effects on the allocation of the outside colony task since $\frac{dx_1^*}{dN} < 0$ and $\frac{dx_2^*}{dN} > 0$. In this



- situation, increasing the colony size, we can expect that the colony increases the allocation to the outside colony task group and decreases the allocation to the inside colony task group.
- 3. If the nonlinear metabolic scaling of the inside colony task δ_1 is larger than the outside colony task δ_2 , i.e., $\delta_2 < \delta_1$, the Eq. (5) implies that the colony size N has positive effects on the allocation of the inside colony task and negative effects on the allocation of the outside colony task since $\frac{dx_1^*}{dN} > 0$ and $\frac{dx_2^*}{dN} < 0$. In this situation, increasing the colony size, we can expect that the colony decreases the allocation to the outside colony task group and increases the allocation to the inside colony task group.

Biological Scenarios 3.21 In the case where work stimulus is greater than the stimulus for rest, the amount of work allocated to inside or outside tasks will vary according to their nonlinear metabolic scaling. That is, the task group with the lowest metabolic scaling will have fewer workers/less work time allocated to them in larger colonies. This scenario assumes that the demand for rest is constant for a given colony size, and lower than the cost of performing tasks. Thus, the remaining amount of work that can be done is split among tasks according to the energetic costs of each task. Effectively, larger colonies will have proportionally more workers allocated to more energetically demanding tasks. Like Biological Scenario 3.11, these effects could represent cases where some tasks have more overhead (or alternatively, are more efficient) than others as colony size scales, and colonies compensating for differences in overhead/efficiency.

3.2.2 Resting demand is constant and greater than task demand

If the relative stimulus of resting $\frac{D_0}{\theta_0} = \Phi N^{\delta_0}$ is larger than that of working \hat{D} , by Theorem 1 the colony rests with the probability $1 - \frac{\hat{D}}{\Phi N^{\delta_0}}$ and works with the probability $\frac{\hat{D}}{\Phi N^{\delta_0}}$ which has the following task allocation:

$$x_1^* = \frac{\hat{D}_1}{\Phi N^{\delta_0}} = \frac{\frac{\gamma_1 N^{\delta_1 - 1}}{\alpha_1 \theta_1}}{\Phi N^{\delta_0}} = \frac{\gamma_1 N^{\delta_1 - \delta_0 - 1}}{\alpha_1 \theta_1 \Phi}$$

and

$$x_2^* = \frac{\hat{D}_2}{\Phi N^{\delta_0}} = \frac{\frac{\gamma_2 N^{\delta_2 - 1}}{\alpha_2 \theta_2}}{\Phi N^{\delta_0}} = \frac{\gamma_2 N^{\delta_2 - \delta_0 - 1}}{\alpha_2 \theta_2 \Phi}.$$

Therefore, we have

$$\frac{dx_1^*}{dN} = \frac{\gamma_1(\delta_1 - \delta_0 - 1)N^{\delta_1 - \delta_0 - 2}}{\alpha_1\theta_1\Phi}, \ \frac{dx_2^*}{dN} = \frac{\gamma_2(\delta_2 - \delta_0 - 1)N^{\delta_2 - \delta_0 - 2}}{\alpha_2\theta_2\Phi},$$

and

$$\frac{dx_0^*}{dN} = -\frac{dx_1^*}{dN} - \frac{dx_2^*}{dN} = \frac{\gamma_1(1+\delta_0-\delta_1)N^{\delta_1-\delta_0-2}}{\alpha_1\theta_1\Phi} + \frac{\gamma_2(1+\delta_0-\delta_2)N^{\delta_2-\delta_0-2}}{\alpha_2\theta_2\Phi}.$$



42 Page 12 of 53 T. Feng et al.

The calculations above indicate the following three scenarios:

1. If the nonlinear metabolic scaling of each task is larger than the sum of the nonlinear metabolic scaling of resting and 1, i.e., $\delta_k > \delta_0 + 1$, we have $\frac{dx_k^*}{dN} > 0$, k = 1, 2, and $\frac{dx_0^*}{dN} < 0$, which indicates that increasing colony size N will increase allocation to all tasks and decrease allocation to resting.

- 2. If the nonlinear metabolic scaling of each task is smaller than the sum of the nonlinear metabolic scaling of resting and 1, i.e., $\delta_k < \delta_0 + 1$, we have $\frac{dx_k^*}{dN} < 0$, k = 1, 2, and $\frac{dx_0^*}{dN} > 0$, which implies that increasing colony size N will decrease allocation to all tasks and increase allocation to resting.
- 3. Assume that $\delta_1 < \delta_0 + 1 < \delta_2$, then we have $\frac{dx_1^*}{dN} < 0$, $\frac{dx_2^*}{dN} > 0$, and

$$\begin{split} \frac{dx_0^*}{dN} &= -\frac{dG(N)}{dN}\frac{1}{\varPhi} = \frac{\gamma_1(\delta_0 + 1 - \delta_1)N^{\delta_1 - \delta_0 - 2}}{\alpha_1\theta_1\varPhi} \\ & \left[1 - \frac{\gamma_2\alpha_1\theta_1(\delta_2 - \delta_0 - 1)N^{\delta_2 - \delta_1}}{\gamma_1\alpha_2\theta_2(\delta_0 + 1 - \delta_1)}\right]. \end{split}$$

According to the Eq. (4), we can conclude that the colony size N has negative effects on the allocation of the inside colony task (k=1) and positive effects on the allocation of the outside colony task (k=2) since $\frac{dx_1^*}{dN} < 0$ and $\frac{dx_2^*}{dN} > 0$. In this situation, as colony size increases, we can expect that the colony increases allocation to the outside task group and decreases allocation to the inside task group. However, the allocation to resting depending on the maturity of the colony.

If a colony is immature, i.e., $N < N_c = \left(\frac{\gamma_1 \alpha_2 \theta_2 (\delta_0 + 1 - \delta_1)}{\gamma_2 \alpha_1 \theta_1 (\delta_2 - \delta_0 - 1)}\right)^{\frac{1}{\delta_2 - \delta_1}}$, increasing the colony size N can decrease the resting allocation, while if a colony is mature, i.e., $N > N_c$, increasing the colony size N can increase the resting allocation.

Biological Scenarios 3.22 If the metabolic scaling for each task is either more or less than resting demand, allocation to rest will either be more or less, as colony size increases. Similarly to Biological Scenario 3.11, this could be explained by the reduction in per capital efficiency due to the reduced communication efficiency (or increased difficulty in accessing tasks) as the colony size increases. However, if the metabolic scaling for one task, e.g., the inside task, is less than that of resting, and the other task, e.g., the outside task is greater, allocation to the inside task should increase and allocation to the outside task decreases as colony size increases. Allocation to resting, however, will depend on colony maturity, where mature colonies will have more allocation to resting than immature colonies.

3.2.3 Resting demand scales with work effort

Assume that the relative stimulus of resting is an increasing function of the working effort $(1 - x_0)$, i.e., $\frac{D_0}{\theta_0} = wN^{\delta_0}(1 - x_0)$. If the relative stimulus of resting wN^{δ_0} is larger than the relative stimulus of working \hat{D} , i.e., $wN^{\delta_0} > \hat{D}$, the colony rests



with the probability $1-\sqrt{\frac{\hat{D}}{wN^{\delta_0}}}$ and works with the probability $\sqrt{\frac{\hat{D}}{wN^{\delta_0}}}$ which has the

$$x_1^* = \frac{\hat{D}_1}{\sqrt{wN^{\delta_0}\hat{D}}} = \frac{\frac{\gamma_1 N^{\delta_1 - 1}}{\alpha_1 \theta_1}}{\sqrt{wN^{\delta_0} \left(\frac{\gamma_1 N^{\delta_1 - 1}}{\alpha_1 \theta_1} + \frac{\gamma_2 N^{\delta_2 - 1}}{\alpha_2 \theta_2}\right)}}$$

and

$$x_{2}^{*} = \frac{\hat{D}_{2}}{\sqrt{wN^{\delta_{0}}\hat{D}}} = \frac{\frac{\gamma_{2}N^{\delta_{2}-1}}{\alpha_{2}\theta_{2}}}{\sqrt{wN^{\delta_{0}}\left(\frac{\gamma_{1}N^{\delta_{1}-1}}{\alpha_{1}\theta_{1}} + \frac{\gamma_{2}N^{\delta_{2}-1}}{\alpha_{2}\theta_{2}}\right)}}.$$

Therefore, we have

$$\frac{dx_i^*}{dN} = \frac{\gamma_i N^{\delta_i - 2} \left(\delta_i - \delta_0 - 1 - \frac{\gamma_j \alpha_i \theta_i (\delta_0 + \delta_j + 1 - 2\delta_i) N^{\delta_j - \delta_i}}{\gamma_i \alpha_j \theta_j} \right)}{2\sqrt{w \gamma_i \alpha_i \theta_i N^{\delta_0 + \delta_i - 1} \left(1 + \frac{\gamma_j \alpha_i \theta_i N^{\delta_j - \delta_i}}{\gamma_i \alpha_j \theta_j} \right) \left(1 + \frac{\gamma_j \alpha_i \theta_i N^{\delta_j - \delta_i}}{\gamma_i \alpha_j \theta_j} \right)}} d\beta_i, \quad (6)$$

and $\frac{dx_0^*}{dN} = -\frac{1}{2}\sqrt{\frac{N^{\delta_0}}{\omega\hat{D}}}\frac{dG(N)}{dt}$. Assume that $\delta_2 \geq \delta_1$, then the calculations above indicate

1. If the inequality $\delta_1 > \frac{\delta_2 + \delta_0 + 1}{2}$ holds, we have

$$\frac{dx_1^*}{dN} > 0$$
, $\frac{dx_2^*}{dN} > 0$ and $\frac{dx_0^*}{dN} < 0$.

Therefore, increasing the colony size, the colony increases the allocation to all the tasks and decreases the allocation to the resting.

2. If the inequality $\delta_2 < \frac{\delta_1 + \delta_0 + 1}{2}$ holds, we have

$$\frac{dx_1^*}{dN} < 0, \ \frac{dx_2^*}{dN} < 0 \text{ and } \frac{dx_0^*}{dN} > 0.$$

Therefore, increasing the colony size, the colony decreases the allocation to all the tasks and increases the allocation to the resting.

3. If the inequality $\delta_0 + 1 < \delta_1 < \frac{\delta_2 + \delta_0 + 1}{2} < \delta_2$ holds, we have $\frac{dx_2^*}{dN} > 0$, $\frac{dx_0^*}{dN} > 0$ and there exists $N_{c1}^1 = \left(\frac{\gamma_1 \alpha_2 \theta_2 (\delta_1 - \delta_0 - 1)}{\gamma_2 \alpha_1 \theta_1 (\delta_2 + \delta_0 + 1 - 2\delta_1)}\right)^{\frac{1}{\delta_2 - \delta_1}}$, such that if $N < N_{c1}^1$, we have

$$\frac{dx_1^*}{dN} > 0.$$

42 Page 14 of 53 T. Feng et al.

In this case, increasing the colony size, the colony increases the allocation to all the tasks and decreases the allocation to the resting. However, if $N > N_{c1}^1$, we have $\frac{dx_1^*}{dN} < 0$, $\frac{dx_2^*}{dN} > 0$ and $\frac{dx_0^*}{dN} > 0$, which implies that when the colony size increases, the allocation to the inside colony task x_1 and the resting decreases, but the allocation to the outside colony task x_2 increases.

4. If the inequality $\delta_1 < \delta_0 + 1 < \delta_2$ holds, we have

$$\frac{dx_1^*}{dN} < 0 \text{ and } \frac{dx_2^*}{dN} > 0,$$

which implies that when the colony size increases, the allocation to the inside colony task x_1 decreases, but the allocation to the outside colony task x_2 increases. Moreover, the allocation to resting depends on the maturity of the colony. By Eq.

(4), if $N < N_c = \left(\frac{\gamma_1 \alpha_2 \theta_2 (\delta_0 + 1 - \delta_1)}{\gamma_2 \alpha_1 \theta_1 (\delta_2 - \delta_0 - 1)}\right)^{\frac{1}{\delta_2 - \delta_1}}$ (e.g., immature colony), increasing the colony size N can increase the allocation of resting, while if $N > N_c$, increasing the colony size N can decrease the allocation of resting.

5. If the inequality $\delta_1 < \frac{\delta_1 + \delta_0 + 1}{2} < \delta_2 < \delta_0 + 1$ holds, we have $\frac{dx_1^*}{dN} < 0$, $\frac{dx_0^*}{dN} > 0$ and there exists $N_{c2}^1 = \left(\frac{\gamma_1 \alpha_2 \theta_2 (2\delta_2 - \delta_1 - \delta_0 - 1)}{\gamma_2 \alpha_1 \theta_1 (\delta_0 + 1 - \delta_2)}\right)^{\frac{1}{\delta_2 - \delta_1}}$, such that if $N > N_{c2}^1$, we have

$$\frac{dx_2^*}{dN} < 0.$$

In this case, increasing the colony size, the colony decreases the allocation to all the tasks and increases the allocation to the resting. However, if $N < N_{c2}^1$, we have $\frac{dx_1^*}{dN} < 0$, $\frac{dx_2^*}{dN} > 0$ and $\frac{dx_0^*}{dN} > 0$, which implies that when the colony size increases, the allocation to the inside colony task x_1 decreases, but the allocation to the outside colony task x_2 and the resting increases.

Biological Scenarios 3.23 In addition to physical needs, inactivity can also result from not having enough work to do (a review for why that might be (Charbonneau and Dornhaus 2015a)). Therefore, the demand/stimulus for inactive may be an increasing function related to the available workforce or available work/colony needs. In this scenario, our theoretical result shows that there are multiple ways in which colony size can affect the allocation of tasks, depending on the level of the nonlinear metabolic scaling and the maturity of the colony (see the results above).

Summary We have been addressing how nonlinear metabolic scaling affects the task allocation and resting probability with respect to changes of the colony size. Our study shows complicated dynamic relationship between the nonlinear metabolic scaling, the colony size, the task allocation, and the resting probability. Our findings have many profound biological significances such as: (1) In the scenario where the resting demand is large enough, if the nonlinear metabolic scaling of the active tasks is large enough, i.e., $\delta_k > \delta_0 + 1$, larger colonies are expected to have a smaller proportion of resting workers. Otherwise, if the nonlinear metabolic scaling of the active tasks



is small enough, i.e., $\delta_k < \delta_0 + 1$, larger colonies are expected to have a larger percentage of resting workers (see Biological Scenarios 3.11). (2) In the scenario where the resting demand is constant and lower than the cost of performing tasks, larger colonies are expected to allocate more workers proportionally to perform more demanding tasks (see Biological Scenarios 3.21). (3) In the scenario where the resting demand is constant and higher than the cost of performing tasks, if the nonlinear metabolic scaling of outside tasks (e.g., foraging) and inside tasks (e.g., breeding) are large and small enough respectively, as the colony size increases, the allocation of outside tasks and inside tasks is expected respectively to increase and decrease (see Biological Scenarios 3.22). (4) In the scenario where the resting demand is increasing with the working effort, if the nonlinear metabolic scaling of inside and outside tasks is large enough, i.e., $\delta_2 > \delta_1 > \frac{\delta_0 + \delta_2 + 1}{2}$, larger colonies are expected to have a greater proportion of workers performing tasks and a smaller proportion of workers resting (see Biological Scenarios 3.23).

4 Dynamics of work activities versus resting

In this section, we apply the modeling framework of System (1) to the case when the number of task groups being 1, i.e., m = 1. This is the case corresponding to studying the task allocation of the working effort x versus resting 1 - x where $x \in [0, 1]$ be the working effort, and $(1 - x) \in [0, 1]$ be the resting. We denote by D the demand of work (or work stimulus), and θ be the response threshold of work. Then we have the following four models:

1. Model I is the case when the resting demand D_0 is a constant function depending on the colony size, i.e., $\frac{D_0}{\theta_0} = \Phi N^{\delta_0}$. We assume that the larger the colony size is, the more the work is needed, thus the resting demand is higher as well.

$$x' = x \left[\frac{\frac{D}{\theta}}{\frac{Dx}{\theta} + \Phi N^{\delta_0} (1 - x)} - 1 \right],$$

$$D' = \gamma N^{\delta} - \alpha N x D.$$
(7)

2. *Model II* is the case when we assume that the resting demand is an increasing function of the working effort x, i.e., $\frac{D_0}{\theta_0} = wxN^{\delta_0}$, which reflects that more work requires more resting to recover.

$$x' = x \left[\frac{\frac{D}{\theta}}{\frac{Dx}{\theta} + wN^{\delta_0}x(1-x)} - 1 \right],$$

$$D' = \chi N^{\delta} - \alpha NxD.$$
(8)



42 Page 16 of 53 T. Feng et al.

3. *Model III* is the case when we assume that the more work a worker does, the more efficient she becomes, and thus her threshold θ for the work decreased to $\frac{\theta}{1+bx}$. We call this model as *The enhanced response threshold model*.

$$x' = x \left[\frac{\frac{\frac{D}{\theta}}{\frac{1}{1+bx}}}{\frac{Dx}{1+bx}} + \Phi N^{\delta_0} (1-x) - 1 \right], \tag{9}$$

$$D' = \nu N^{\delta} - \alpha N x D.$$

4. *Model IV* is the case that we assume that the working demand has a carrying capacity KN^{δ} .

$$x' = x \left[\frac{\frac{D}{\theta}}{\frac{Dx}{\theta} + \Phi N^{\delta_0} (1 - x)} - 1 \right],$$

$$D' = \gamma N^{\delta} \left(1 - \frac{D}{K N^{\delta}} \right) - \alpha N x D.$$
(10)

The dynamics of Models I–IV can be summarized by the following theorem:

Theorem 2 (Summary of dynamics) *The dynamics of Models I–IV is summarized in Table 1. Moreover, for Model III-*The enhanced response threshold model, *its interior equilibrium* $\hat{E}^* = (\hat{x}^*, \hat{D}^*)$ *is locally asymptotically stable if* $N \geq \frac{b}{\alpha}$, *while if* $N < \frac{b}{\alpha}$ *we have the following results:*

- 1. Let Φ be the bifurcation parameter: \hat{E}^* is locally asymptotically stable if $\Phi < \Phi^*$, while it is unstable if $\Phi > \Phi^*$, and a Hopf bifurcation occurs at $\Phi = \Phi^*$, where $\Phi^* = \frac{\gamma b(1+b)N^{\delta-\delta_0-1}}{\alpha\theta(b-\alpha N)}$.
- 2. Let b be the bifurcation parameter: (1) when $\Delta = (\gamma N^{\delta-\delta_0-1} \Phi\alpha\theta)^2 4\gamma\alpha^2\Phi\theta N^{\delta-\delta_0} < 0$, \hat{E}^* is locally asymptotically stable; (2) when $\Delta > 0$, \hat{E}^* is locally asymptotically stable if $b < b_1^*$ or $b > b_2^*$, while it is unstable if $b_1^* < b < b_2^*$, and two Hopf bifurcations occur at b_1^* and b_2^* , respectively, where $b_1^* = \frac{\Phi\alpha\theta \gamma N^{\delta-\delta_0-1} \sqrt{\Delta}}{2\gamma N^{\delta-\delta_0-1}}$ and $b_2^* = \frac{\Phi\alpha\theta \gamma N^{\delta-\delta_0-1} + \sqrt{\Delta}}{2\gamma N^{\delta-\delta_0-1}}$.
- 3. Let N be the bifurcation parameter: (1) when $\delta > \delta_0 + 1$, \hat{E}^* is unstable if $N < N^*$, while it is locally asymptotically stable if $N > N^*$, and a Hopf bifurcation occurs at $N = N^*$, where N^* is the unique positive root of function $f(N) = b(1+b)\gamma N^{\delta-\delta_0-1} + \alpha^2 \Phi \theta N \alpha b \Phi \theta = 0$; (2) when $\delta < \delta_0 + 1$, we have:
 - (a) if $N_1 = \frac{\alpha^2 \Phi \theta}{(1+\delta_0-\delta)b(1+b)\gamma}^{\frac{1}{\delta-\delta_0-2}} < N_0 = \frac{\Phi \alpha \theta}{\gamma(1+b)}^{\frac{1}{\delta-\delta_0-1}} \text{ or } N_1 > N_0, f(N_1) > 0,$ \hat{E}^* is locally asymptotically stable;
 - (b) if $N_1 > N_0$ and $f(N_1) < 0$: \hat{E}^* is locally asymptotically stable if $N < N_1^*$ or $N > N_2^*$, while it is unstable if $N \in (N_1^*, N_2^*)$, and two Hopf bifurcations



occur at $N = N_1^*$ and $N = N_2^*$, respectively, where N_1^* , N_2^* are the positive roots of function f(N) = 0.

Notes The proof of Theorem 2 is given in Sect. 7. Theorem 2 shows us the global dynamics of Models I–IV. It shows that Models I, II, and IV have only equilibrium dynamics, while Model III-*The enhanced response threshold model* has both equilibrium dynamics and periodic dynamics. In addition, we provide the following findings:

- 1. The dynamics of Model I can be determined by the value of resting demand. If $\Phi < \frac{\gamma N^{\delta-\delta_0-1}}{\alpha\theta}$, Model I has a unique equilibrium E^* which is globally asymptotically stable. Otherwise, if $\Phi > \frac{\gamma N^{\delta-\delta_0-1}}{\alpha\theta}$, E^* is unstable, and Model I has an interior equilibrium \hat{E}^* which is globally asymptotically stable. This result suggests that: if the resting demand is small enough, i.e., $\Phi < \frac{\gamma N^{\delta-\delta_0-1}}{\alpha\theta}$, the colony works all the time, i.e., x = 1 (see area A1 of Fig. 1a). Otherwise, if the resting demand is large enough, i.e., $\Phi > \frac{\gamma N^{\delta-\delta_0-1}}{\alpha\theta}$, the colony rests at a certain level (see area A2 of Fig. 1a). By Theorem 2, the working level $\hat{x}^* = \frac{\gamma N^{\delta-\delta_0-1}}{\Phi\alpha\theta}$ is decreasing with respect to the resting demand, is decreasing with respect to the colony size if $\delta < \delta_0 + 1$, and is increasing with respect to the colony size if $\delta < \delta_0 + 1$. This result indicates that: (i) the larger the resting demand, the workers work less (see area A2 of Fig. 1a); (ii) if the metabolic scaling of work is large enough, i.e., $\delta > \delta_0 + 1$, the larger colony size N, the workers work more (see Fig. 1b, this result is consistent with the results of Schmid-Hempel 1990), while if the metabolic scaling is small enough, i.e., $\delta < \delta_0 + 1$, the larger colony size N, the workers work less (Fig. 1c, which echoes the results of Houston et al. 1988 and Franks and Partridge 1993).
- 2. The global dynamics of Model II are very similar to that of Model I, so we will not go into details here. The readers can see the full dynamics of Model II through Fig. 2. The only difference between Model I and Model II is that when the resting demand is large enough, the resting ratio of Model I $(1 x^*)$ is lower than the resting ratio of Model II $(1 \sqrt{x^*})$.
- 3. Model IV always has a working-free equilibrium E_0^* and a resting-free equilibrium E_1^* , and can have an interior equilibrium \hat{E}^* under certain conditions. The global dynamics of Model IV is determined by the value of resting demand Φ : if $\Phi < \frac{KN^{\delta-\delta_0}}{\theta} \frac{\gamma}{\gamma+\alpha KN}$, E_0^* being unstable and E_1^* being globally asymptotically stable; if $\Phi > \frac{KN^{\delta-\delta_0}}{\theta}$, E_0^* being globally asymptotically stable and E_1^* being unstable. Otherwise, if $\frac{KN^{\delta-\delta_0}}{\theta} \frac{\gamma}{\gamma+\alpha KN} < \Phi < \frac{KN^{\delta-\delta_0}}{\theta}$, E_0^* and E_1^* are unstable and Model IV has an interior equilibrium \hat{E}^* which is globally asymptotically stable. This analytical result suggests that: if the resting demand is small enough, i.e., $\Phi < \frac{KN^{\delta-\delta_0}}{\theta} \frac{\gamma}{\gamma+\alpha KN}$, the colony works all the time, i.e., x=1 (see area A1 of Fig. 3a); if $\frac{KN^{\delta-\delta_0}}{\theta} \frac{\gamma}{\gamma+\alpha KN} < \Phi < \frac{KN^{\delta-\delta_0}}{\theta}$, the colony rests at a certain level, i.e., $0 < x_0 < 1$ (see area A2 of Fig. 3a). Otherwise, if the resting demand is large enough, i.e., $\Phi > \frac{KN^{\delta-\delta_0}}{\theta}$, the colony rests all the time, i.e., $x_0 = 1$ (see area A3 of Fig. 3a). By Theorem 2, when \hat{E}^* exists, the workers working at the level $\hat{x}^* = \frac{\gamma(KN^{\delta-\delta_0}-\Phi\theta)}{K\alpha\Phi\theta N}$, indicating that: (i) the larger the resting demand, the colony



Table 1 Existence and stability of equilibria where GAS is an abbreviation for globally asymptotically stable

	•	•	
Models	Equilibria	Existence condition	Stability condition
I	$E^*(1,\frac{\gamma N^{\delta-1}}{\alpha})$	Always	GAS if $\phi < \frac{\gamma N^{\delta - \delta_0 - 1}}{\alpha \theta}$,
	$\hat{E}^*(rac{ u^{N\delta-\delta_0-1}}{\phi_{lpha heta}}, \sigma heta N^{\delta_0})$	$\Phi > rac{{ u N^{\delta - \delta_0 - 1}}}{{lpha heta}}$	GAS.
п	$E^*(1,rac{ u N^{\delta-1}}{lpha})$	Always	GAS if $\omega < \frac{\gamma N^{\delta - \delta_0 - 1}}{\alpha \theta}$,
	$\hat{E}^*(\sqrt{\frac{\nu N^{5-30-1}}{u\alpha\theta}},\sqrt{\frac{w\gamma\theta N^{3+50-1}}{\alpha}})$	$\omega > \frac{\gamma N^{\delta - \delta_0 - 1}}{\alpha \theta}$	GAS.
Ш	$E^*(1,rac{arkappa N \delta^{-1}}{lpha})$	Always	GAS if $\phi < \frac{\gamma(1+b)N^{\delta-\delta_0-1}}{\alpha\theta}$,
	$\hat{E}^*(rac{\gamma N^{\delta-\delta_0-1}}{\phi_{lpha heta-b\gamma N^{\delta-\delta_0-1}}}, \Phi heta N^{\delta_0} - rac{b\gamma N^{\delta-1}}{lpha})$	$\phi > rac{\gamma(1+b)N^{\delta-\delta_0-1}}{lpha heta}$	See Theorem 2.
IV	$E_0^*(0,KN^\delta)$	Always	GAS if $\Phi > \frac{KN^{\delta - \delta_0}}{\theta}$,
	$E_1^*(1,rac{K\gamma N^\delta}{lpha KN+\gamma})$	Always	GAS if $\Phi < \frac{KN^{\delta-\delta_0}}{\theta} \frac{\gamma}{\gamma + \alpha KN}$,
	$\hat{E}^*(rac{\gamma \left(KN^{\delta-\delta 0}-\phi heta ight)}{K\phi lpha heta N}, \phi heta N^{\delta 0})$	$\frac{KN^{\delta-\delta_0}}{\theta} \frac{\gamma}{\gamma + \alpha KN} < \Phi < \frac{KN^{\delta-\delta_0}}{\theta}$	GAS.

where GAS is an abbreviation for globally asymptotically stable



works less; (ii) if the metabolic scaling is large enough, i.e., $\delta > \delta_0 + 1$, the larger colony size N, the workers work more (see area A2 of Fig. 3b); (iii) if the metabolic scaling is small enough, i.e., $\delta < \delta_0 + 1$, the relationship between colony size and the working activity depends on the value of colony size: when the colony size is small enough, i.e., $N \leq \frac{\Phi\theta}{K(1+\delta_0-\delta)}^{\frac{1}{\delta-\delta_0}}$, the larger colony size N, the workers work more (see area A2 of Fig. 3c); when the colony size is large enough, i.e., $N > \frac{\Phi\theta}{K(1+\delta_0-\delta)}^{\frac{1}{\delta-\delta_0}}$, the larger colony size N, the workers work less (see area A4 of Fig. 3c). Note that Model IV can be derived from Model II by adding a carrying capacity for the working demand. When the carrying capacity $\frac{K}{\gamma}$ is large enough, we can approximate $\gamma + \alpha K N$ to $\alpha K N$, and therefore $\frac{KN^{\delta-\delta_0}}{\theta} \frac{\gamma}{\gamma + \alpha K N} \approx \frac{\gamma N^{\delta-\delta_0-1}}{\alpha \theta}$. In this situation, Model II and Model IV have similar dynamics. However, when the carrying capacity is not large enough, Model II and Model IV have different dynamics: if the resting demand is large enough, the colony of Model II would do resting at a certain ratio (see area A2 of Fig. 2a), while the colony of Model IV rests all the time (see area A3 of Fig. 3a).

4. Model III - The enhanced response threshold model has rich dynamics. If the resting demand is small enough, i.e., $\Phi < \frac{\gamma(1+b)N^{\delta-\delta_0-1}}{\alpha\theta}$, the colony works all the time, i.e., x=1 (see area A1 of Fig. 4a, b). If the resting demand is large enough but the colony size is not very large, i.e., $\Phi > \frac{\gamma(1+b)N^{\delta-\delta_0-1}}{\alpha\theta}$ and $N < \frac{b}{\alpha}$, the colony rests in varied patterns (see areas A2 and A3 of Fig. 4a, c, d). Otherwise, if the resting demand and colony size are large enough, i.e., $\Phi > \frac{\gamma(1+b)N^{\delta-\delta_0-1}}{\alpha\theta}$ and $N > \frac{b}{\alpha}$, the colony rests in equilibrium patterns (see area A2 of Fig. 4b).

By Theorem 2 and the simulations, the working level $\hat{x}^* = \frac{\gamma N^{\delta - \delta_0 - 1}}{\phi \alpha \theta - b \gamma N^{\delta - \delta_0 - 1}}$ is increasing with respect to the colony size if \hat{x} in \hat{x} increasing with respect to the colony size if $\delta > \delta_0 + 1$ and is decreasing with respect to the colony size if $\delta < \delta_0 + 1$. This result suggests that: (i) if the metabolic scaling is large enough, i.e., $\delta > \delta_0 + 1$, the larger colony size N, the workers work more, and the colony works in varied patterns (Fig. 5a); (ii) if the metabolic scaling is small enough, i.e., $\delta < \delta_0 + 1$, the larger colony size N, the workers work less, and the intermediate values of N destabilize the system (Fig. 5b). In addition, Theorem 2 shows that the threshold regulator b has a significant effect on the dynamics of Model III: (i) the working level \hat{x} is increasing with respect to the threshold regulator b, indicating that the larger threshold regulator b, the workers work more; (ii) under the conditions of Theorem 2 2(2), the interior equilibrium E^* is locally stable if $b < b_1^*$ or $b > b_2^*$ and is unstable if $b_1^* < b < b_2^*$, indicating that the intermediate values of b destabilize the system (Fig. 6). The dynamic process looks like a bubble, so it is called bubble phenomenon by Liu et al. 2015. This is the first time we observed bubbles in the dynamics of social insect colonies; and (iii) when the threshold regulator of Model III becomes zero, i.e., b = 0, Model III becomes the same as Model I. Note that Model I has only equilibrium dynamics and Model III has rich dynamics, which means that the enhanced response threshold b can destabilize the equilibrium and lead to periodic dynamics.



42 Page 20 of 53 T. Feng et al.

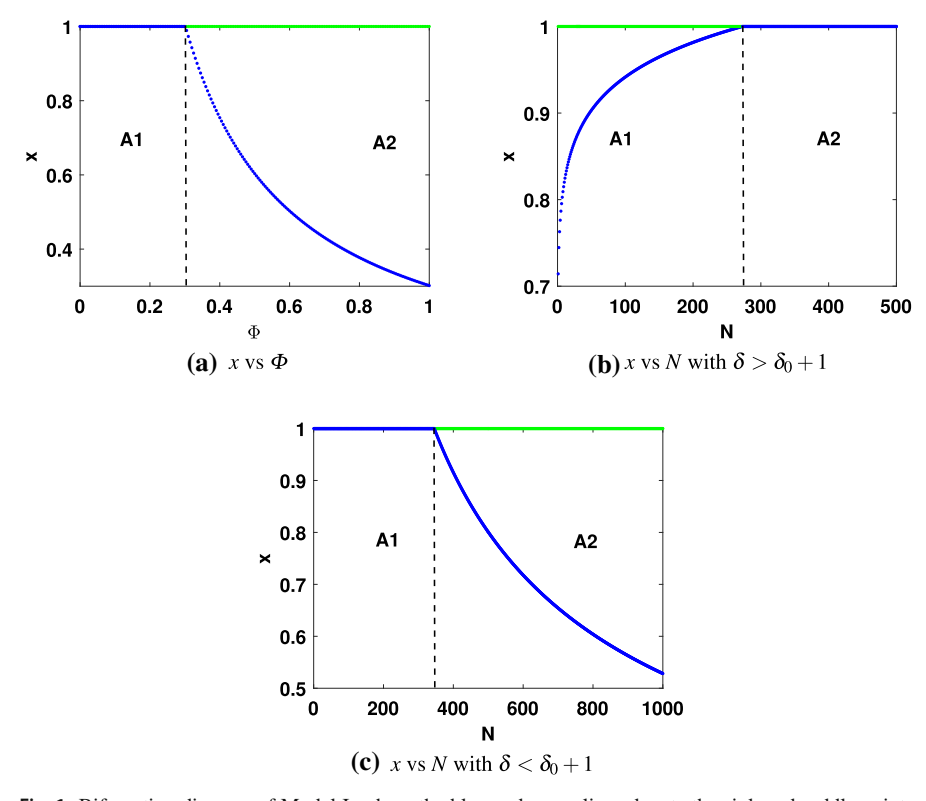


Fig. 1 Bifurcation diagram of Model I, where the blue and green lines denote the sink and saddle points, respectively. In Fig. 1a, the parameters are given by $\theta=0.1,\,\delta_0=0.3,\,\gamma=1,\,\alpha=0.2,\,N=5000,\,\delta=0.7.$ In area A1, Model I has a unique equilibrium E^* which is globally asymptotically stable. In area A2, E^* is unstable, and Model I has an interior equilibrium \hat{E}^* which is globally asymptotically stable. In Fig. 1b, the parameters are given by $\theta=0.8,\,\delta_0=0.01,\,\gamma=0.3,\,\alpha=0.35,\,\Phi=1.5,\,\delta=1.07.$ In area A1, Model I has two equilibria: E^* being unstable and \hat{E}^* being globally asymptotically stable. In area A2, Model I has a unique equilibrium E^* which is globally asymptotically stable. In Fig. 1c, the parameters are given by $\theta=0.2,\,\delta_0=0.3,\,\gamma=0.5,\,\alpha=0.15,\,\Phi=0.5,\,\delta=0.7.$ In area A1, Model I has a unique equilibrium E^* which is globally asymptotically stable. In area A2, E^* is unstable, and Model I has an interior equilibrium \hat{E}^* which is globally asymptotically stable

Summary: The theoretical and bifurcation analyses conducted in this section address the first two questions that we proposed in the introduction part: (i) how does the metabolic scaling affect the task allocation and resting probability of social insect colonies, as colony size increases? (ii) how does the colony size affect the working activity in different scenarios of working versus resting?

Based on our study, the colony size, metabolic rates and the demand for resting are working in synergistic and nonlinear ways to generate interesting task allocation dynamics. Some of the biological insights that we could illustrate here are: (1) More demand for the work, then workers of the colony work more. In the case that the colony size is small, then large demand may destabilize the system (see *The enhanced response threshold model*). (2) If the metabolic scaling of work is large enough, i.e., $\delta > \delta_0 + 1$, the larger colony size N, the workers work more; while if the metabolic



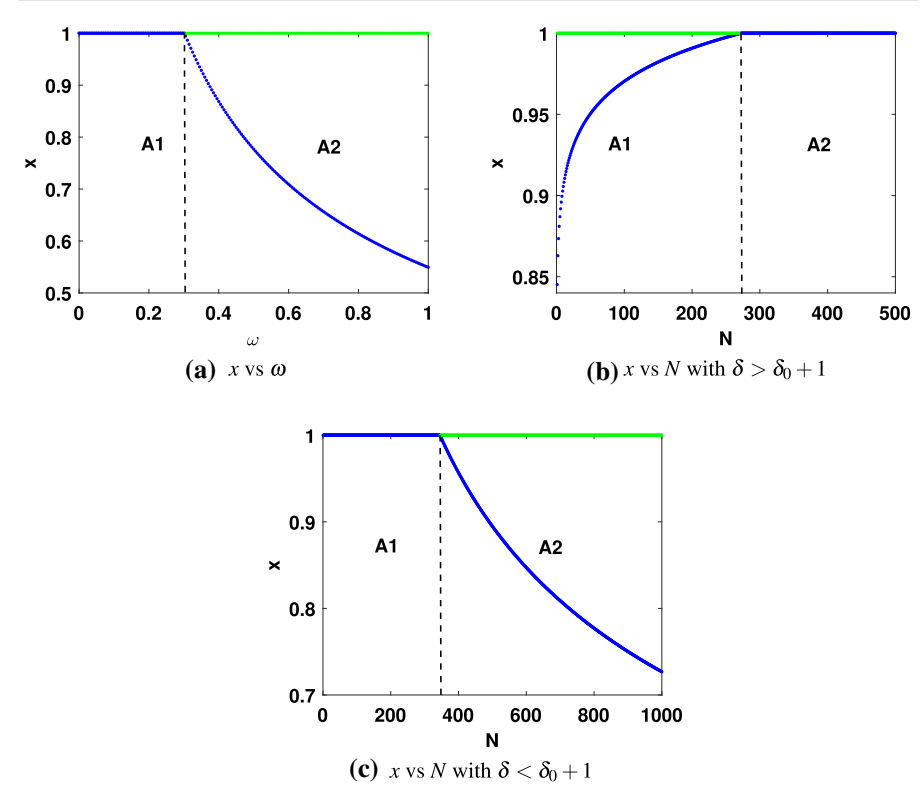


Fig. 2 Bifurcation diagram of Model II, where the blue and green lines denote the sink and saddle points, respectively. In Fig. 2a, the parameters are given by $\theta=0.1$, $\delta_0=0.3$, $\gamma=1$, $\alpha=0.2$, N=5000, $\delta=0.7$. In area A1, Model II has a unique equilibrium E^* which is globally asymptotically stable. In area A2, E^* is unstable, and Model II has an interior equilibrium \hat{E}^* which is globally asymptotically stable. In Fig. 2b, the parameters are given by $\theta=0.8$, $\delta_0=0.01$, $\gamma=0.3$, $\alpha=0.35$, $\omega=1.5$, $\delta=1.07$. In area A1, Model II has two equilibria: E^* being unstable and \hat{E}^* being globally asymptotically stable. In area A2, Model II has a unique equilibrium E^* which is globally asymptotically stable. In Fig. 2c, the parameters are given by $\theta=0.2$, $\delta_0=0.3$, $\gamma=0.5$, $\alpha=0.15$, $\omega=0.5$, $\delta=0.7$. In area A1, Model II has a unique equilibrium E^* which is globally asymptotically stable. In area A2, E^* is unstable, and Model II has an interior equilibrium \hat{E}^* which is globally asymptotically stable

scaling is small enough, i.e., $\delta < \delta_0 + 1$, the larger colony size N, the workers work less or work more at the beginning but less when the colony size is really large. And (3) the small size colony is prone to have fluctuating dynamics when the metabolic scaling of work is large enough, i.e., $\delta > \delta_0 + 1$; while the intermediate size colony seems to have fluctuating dynamics when $\delta < \delta_0 + 1$ (please see the dynamics of Model III as an example).

5 Effects of random noise on task allocation and demand

In this section, we explore how random noise affects the dynamics of task allocation and demand by taking Model III and IV as examples. We investigate three



42 Page 22 of 53 T. Feng et al.

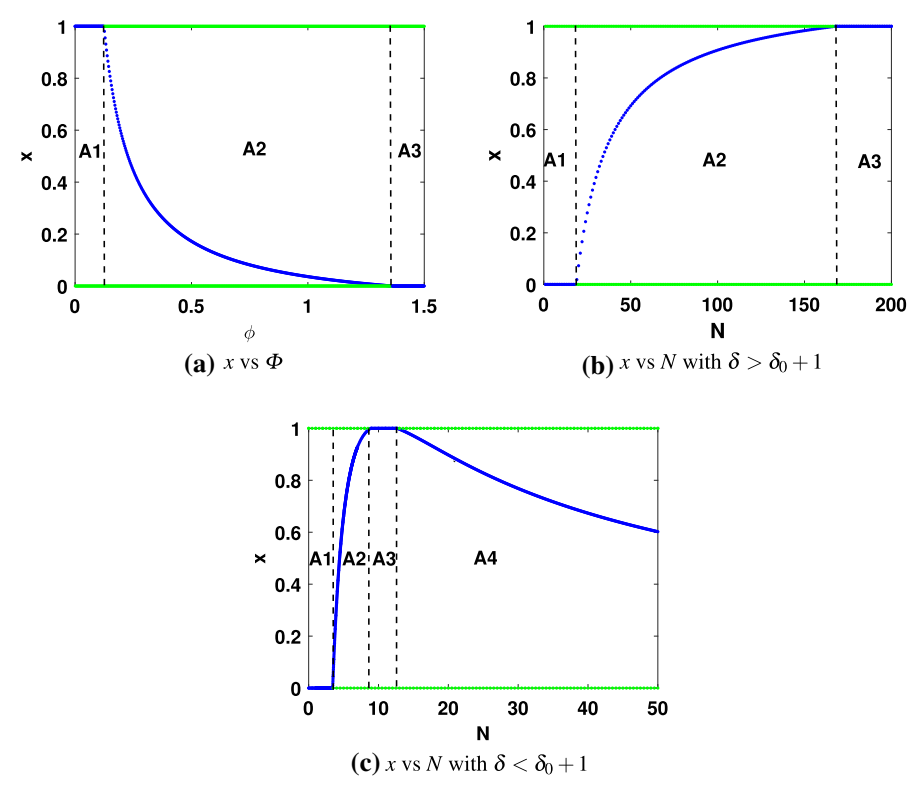


Fig. 3 Bifurcation diagram of Model IV, where the blue and green lines represent the sink and saddle points, respectively. In Fig. 3a, the parameters are given by $\theta=3.6$, $\delta_0=0.4$, $\gamma=1$, $\alpha=0.05$, K=1, N=200, $\delta=0.7$. In area A1, E_1^* is globally asymptotically stable and E_0^* is unstable. In area A2, E_0^* and E_1^* are unstable and Model IV has an interior equilibrium \hat{E}^* which is globally asymptotically stable. In area A3, E_0^* is globally asymptotically stable and E_1^* is unstable. In Fig. 3b, the parameters are given by $\theta=3.6$, $\delta_0=0.05$, $\gamma=1$, $\alpha=0.05$, $\phi=5.5$, K=1, $\delta=1.07$. In area A1, E_0^* is globally asymptotically stable and E_1^* is unstable. In area A2, E_0^* and E_1^* are unstable and Model IV has an interior equilibrium \hat{E}^* which is globally asymptotically stable. In area A3, E_1^* is globally asymptotically stable and E_0^* is unstable. In Fig. 3c, the parameters are given by $\theta=0.4$, $\delta_0=0.6$, $\gamma=8.5$, $\alpha=0.2$, $\phi=3.2$, K=1, $\delta=0.8$. In area A1, E_0^* is globally asymptotically stable and E_1^* is unstable. In area A2 and A4, E_0^* and E_1^* are unstable and Model IV has an interior equilibrium \hat{E}^* which is globally asymptotically stable. In area A3, E_1^* is globally asymptotically stable and E_0^* is unstable. In area A3, E_1^* is globally asymptotically stable and E_0^* is unstable. In area A3, E_1^* is globally asymptotically stable and E_0^* is unstable.

cases based on the dynamics of Models III and IV respectively (see Theorem 2). Specifically, for Model III: (i) Model III has a unique resting-free equilibrium $E^*(1, \frac{\gamma N^{\delta-1}}{\alpha})$ which is global asymptotically stable; (ii) Model III has two equilibria: the resting-free equilibrium $E^*(1, \frac{\gamma N^{\delta-1}}{\alpha})$ being unstable and the interior equilibrium $\hat{E}^*(\frac{\gamma N^{\delta-\delta_0-1}}{\Phi\alpha\theta-b\gamma N^{\delta-\delta_0-1}}, \Phi\theta N^{\delta_0} - \frac{b\gamma N^{\delta-1}}{\alpha})$ being locally asymptotically stable; and (iii) Model III has a periodic solution.

Similarly, for Model IV: (i) Model IV has two equilibria: the working free equilibrium $E_0^*(0, KN^\delta)$ being unstable and the resting free equilibrium $E_1^*(1, \frac{K\gamma N^\delta}{\alpha KN + \gamma})$



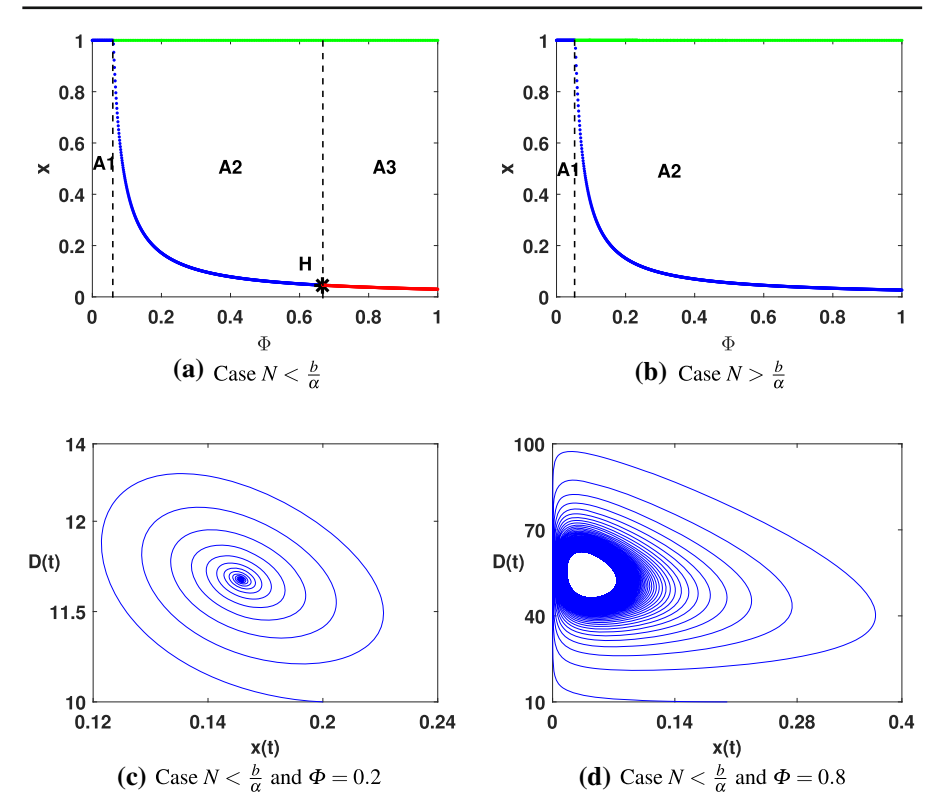


Fig. 4 Bifurcation diagrams and phase portraits of **Model III**- The enhanced response threshold model with parameters $\theta=5$, $\delta_0=0.5$, $\gamma=0.05$, $\alpha=0.005$, $\delta=0.7$, b=1.1, where H denotes the Hopf bifurcation point. In Fig. 4a and b, the blue, red and green lines denote the sink, source and saddle points, respectively. In Fig. 4a, we choose N=200. Area A1 indicates that Model III has a unique equilibrium E^* which is globally asymptotically stable. Area A2 indicates that E^* is unstable and Model III has an interior equilibrium \hat{E}^* which is globally asymptotically stable. In area A3, E^* and \hat{E}^* are unstable and Model III has a periodic solution. In Fig. 4b, we choose N=230. Area A1 indicates that Model III has a unique equilibrium E^* which is globally asymptotically stable. Area A2 indicates that E^* is unstable and Model III has an interior equilibrium \hat{E}^* which is globally asymptotically stable. In Fig. 4c, we choose N=200 and $\Phi=0.2$, it shows that the unique interior equilibrium \hat{E}^* is locally asymptotically stable. In Fig. 4d, we choose N=200 and $\Phi=0.8$, it shows that the unique interior equilibrium \hat{E}^* is unstable and a periodic orbit occurs

being globally asymptotically stable; (ii) Model IV has three equilibria: E_0^* , E_1^* being unstable and the interior equilibrium $\hat{E}^*(\frac{\gamma(KN^{\delta-\delta_0}-\Phi\theta)}{K\Phi\alpha\theta N},\Phi\theta N^{\delta_0})$ being globally asymptotically stable; and (iii) Model IV has two equilibria: E_1^* being unstable and E_0^* being globally asymptotically stable.

Our numerical results are obtained using the Euler-Maruyama method (Higham 2001) and Matlab 2019b with the step size given by $\Delta t = 10^{-3}$. The parameters for the following simulations are shown in Table 2.



42 Page 24 of 53 T. Feng et al.

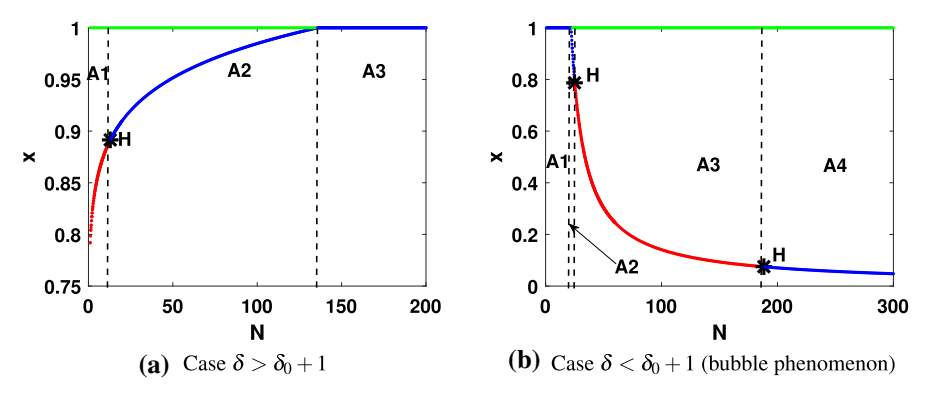


Fig. 5 Bifurcation diagram of Model III-The enhanced response threshold model, where H denotes the Hopf bifurcation point, the blue, red and green lines denote the sink, source and saddle points, respectively. In Fig. 5a, we choose $\theta=0.113$, $\Phi=0.5$, $\gamma=0.00011$, b=1.1, $\alpha=0.0046$, $\delta_0=0.046$, $\delta=1.07$. Area A1 indicates that the equilibria E^* and \hat{E}^* are unstable and Model III has a periodic solution. Area A2 indicates that E^* is unstable and Model III has an interior equilibrium \hat{E}^* which is globally asymptotically stable. In area A3, Model III has a unique equilibrium E^* which is globally asymptotically stable. In Fig. 5b, we choose $\theta=2.6$, $\Phi=1$, $\gamma=0.1$, b=1.1, $\alpha=0.05$, $\delta_0=0.6$, $\delta=0.7$. Area A1 indicates that Model III has a unique equilibrium E^* which is globally asymptotically stable. Areas A2 and A4 indicate that E^* is unstable and Model III has an interior equilibrium E^* which is globally asymptotically stable. Area A3 indicates that the equilibria E^* and E^* are unstable and Model III has a periodic solution

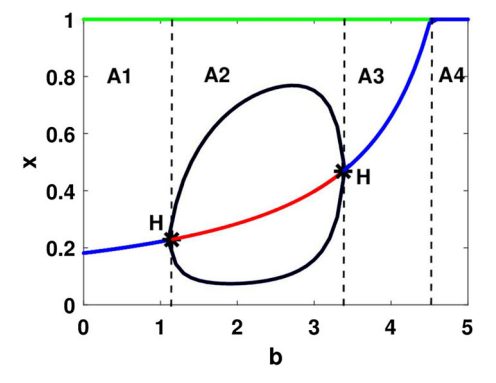


Fig. 6 Bifurcation diagram of Model III- The enhanced response threshold model with $\Phi=5$, $\theta=5$, N=200, $\delta_0=0.7$, $\gamma=1.1$, $\delta=0.9$, $\alpha=0.0035$, where H represents the Hopf bifurcation point, the blue, red and green lines denote the sink, source and saddle points, respectively. In areas A1 and A3, E^* is unstable and the unique equilibrium \hat{E}^* is locally asymptotically stable. In area A2, E^* (green line) and \hat{E}^* (red line) are unstable and Model III has a periodic solution (the black curves denote the maximum and minimum values of the periodic solution, respectively). In area A4, the unique equilibrium E^* is globally asymptotically stable. The dynamic process looks like a bubble, so it was named as bubble phenomenon by Liu et al. 2015

5.1 Case study: the enhanced response threshold Model

Assume that the random noise affects task demand of social insect colonies, and thus affects the whole colony dynamics. From the full system (2), we obtain the stochastic version of Model III as follows:



Parameter		Model III	Model IV
θ	Response threshold of working	5	3.6
δ_0	Nonlinear metabolic scaling of resting	0.5	0.4
δ	Nonlinear metabolic scaling of working	0.7	0.7
γ	The increase in demand intensity per unit time for working	0.05	1
α	Performance efficiency of working	0.005	0.05
N	Colony size	200	200
b	Strength of enhancement	1.1	Null
K	Carrying capacity of working demand	Null	1
Φ	Resting demand	Variable	Variable
σ	Intensity of noise	Variable	Variable

Table 2 Parameters for the simulations of case studies 5.1 and 5.2

$$dx(t) = x \left[\frac{\frac{D}{\frac{\theta}{\theta}}}{\frac{Dx}{\theta + \Phi} N^{\delta_0} (1 - x)} - 1 \right] dt, \tag{11}$$

$$dD(t) = (\gamma N^{\delta} - \alpha N x D) dt + \sigma D(t) dB(t),$$

where σ^2 is the intensity of random noise, B(t) is a standard one-dimensional independent Brownian motion defined on the complete probability space $(\Omega, \mathscr{F}, \mathbb{P})$. We performed numerical simulations for cases $\delta - \delta_0 - 1 > 0$ (not shown here) and $\delta - \delta_0 - 1 < 0$, respectively. The results show that the size of $\delta - \delta_0 - 1$ does not affect the way the noise affects the work activity and the task command, so we only show the numerical results of case $\delta - \delta_0 - 1 < 0$ here. By Theorem 2, the dynamics of Model III can be summarized into the following three scenarios:

- (a) If Φ < 0.06, Model III has a unique resting-free equilibrium $E^* = (x^*, D^*) = (1, 2.04)$ which is globally asymptotically stable.
- (b) If $0.06 < \Phi < 0.67$, Model III has two equilibria: E^* being unstable and

$$\hat{E}^* = (\hat{x}^*, \hat{D}^*) = \left(\frac{0.72}{25\Phi - 0.79}, 70.71\Phi - 2.24\right)$$

being locally asymptotically stable.

(c) If $\Phi > 0.67$, the equilibria E^* and \hat{E}^* are unstable and there is a periodic solution.

Next, we study the effects of random fluctuations on task allocation and demand in scenarios (a), (b) and (c), respectively.

We first consider the scenario (a). By choosing $\Phi = 0.055$, we obtain results in Fig. 7 showing that: (i) the resting-free equilibrium $E^*(x^*, D^*) = (1, 2.04)$ of the deterministic form of Model III is globally asymptotically stable (red lines), this is in line with the theoretical results of Theorem 2; (ii) the empirical mean x(t) (over 500)



42 Page 26 of 53 T. Feng et al.

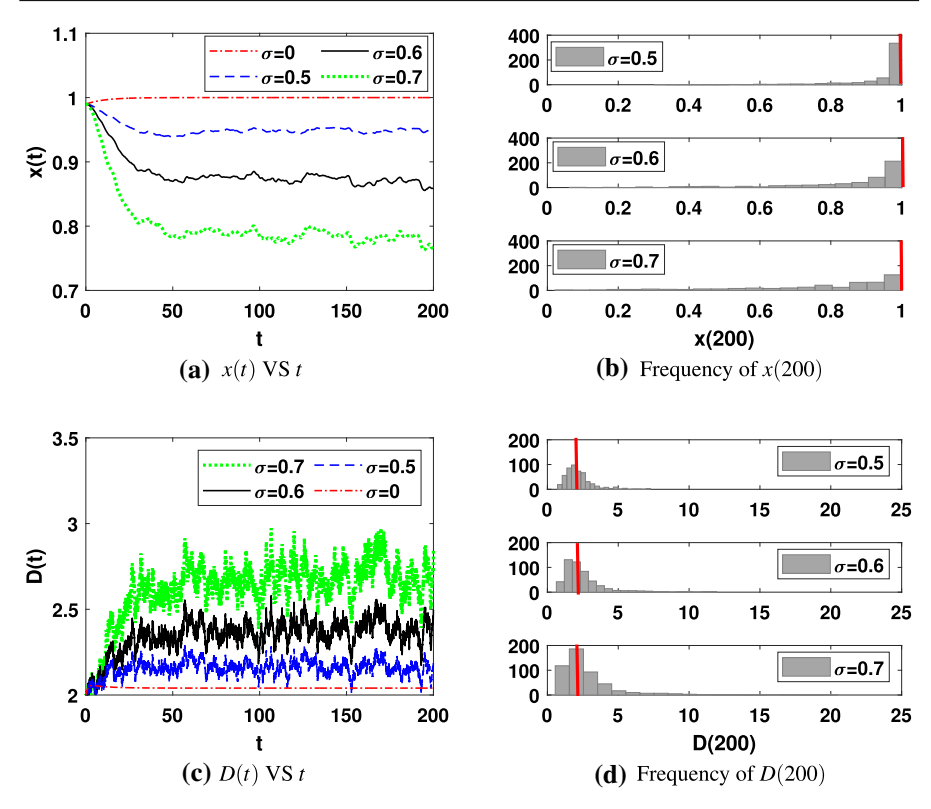


Fig. 7 Empirical mean and frequency of Model (11) and Model III with $\Phi=0.055$ over 500 replicates. The other parameters are given by $\theta=5$, b=1.1, $\delta_0=0.5$, $\gamma=0.05$, $\delta=0.7$, $\alpha=0.005$, N=200, x(0)=0.99, D(0)=2. Red line indicates the solution of Model III, blue, black and green lines denote the empirical mean of the stochastic solution with $\sigma=0.5$, 0.6 and 0.7, respectively. Figure 7b, d are the frequency of Model (11) at time t=200

replicates) of Model (11) fluctuates below x^* (Fig. 7a), while the empirical mean D(t) of Model (11) fluctuates above D^* (Fig. 7c); (iii) the amplitude of the fluctuation is positively correlated with the intensity of stochastic noise σ ; and (iv) when the time is large enough, the variance of the frequency of the stochastic solution (over 500 replicates) is positively correlated with the intensity of the noise (see Fig. 7b, d). The simulation result suggests that: although random fluctuation leads to an increase in average for task demand D, the working activity x of the colony decreases in average over 500 replicates.

Next, we study the scenario (b) by choosing $\Phi = 0.07$. It follows from Theorem 2 that the unique interior equilibrium $\hat{E}^*(\hat{x}^*, \hat{D}^*) = (0.72, 2.71)$ of Model III is global asymptotically stable (see red lines in Fig. 8). Figure 8 indicates that the effects of random fluctuations on the task allocation and demand in scenario (b) are similar to that in scenario (a). Particularly, Figures 7b, d and 8b, d imply that there appears to be a stationary distribution of the stochastic system (see, for example Cai et al. 2015;



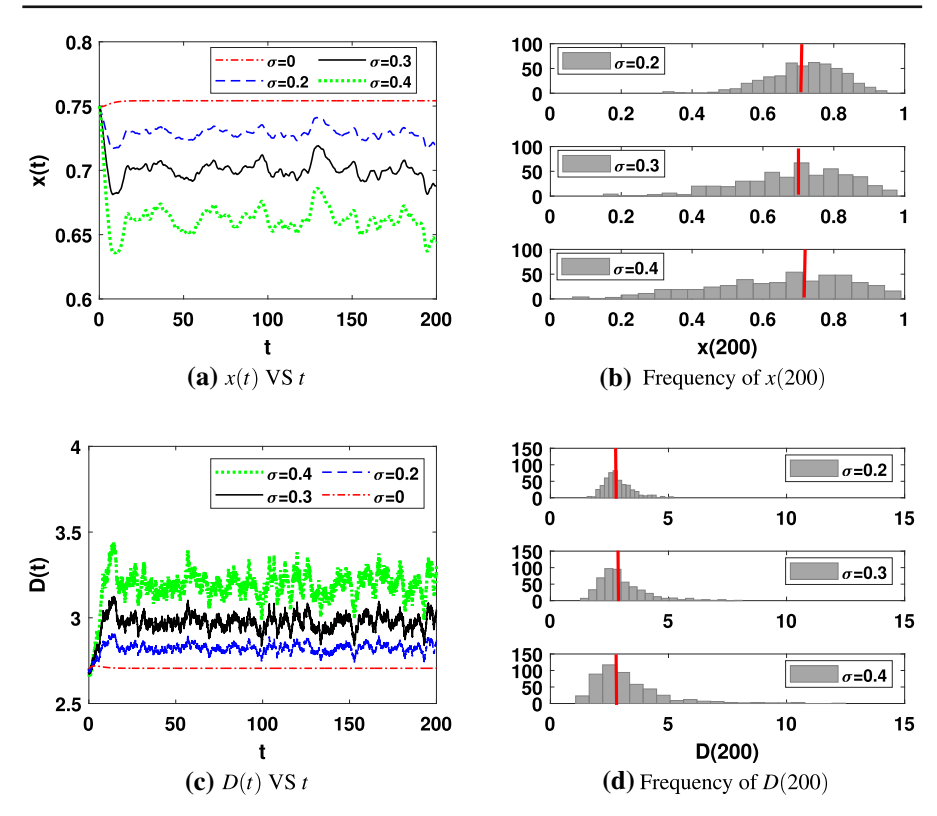


Fig. 8 Empirical mean and frequency of Model (11) and Model III with $\Phi = 0.07$ over 500 replicates. The other parameters are given by $\theta = 5$, b = 1.1, $\delta_0 = 0.5$, $\gamma = 0.05$, $\delta = 0.7$, $\alpha = 0.005$, N = 200, x(0) = 0.75, D(0) = 2.7. Red line indicates the solution of Model III, blue, black and green lines indicate the empirical mean of the stochastic solution (x(t), D(t)) with $\sigma = 0.2$, 0.3 and 0.4. Figures 8b, d are the frequency of Model (11) at time t = 200

Feng et al. 2019). It would be a future work to prove the existence of this stationary distribution theoretically.

Finally, we study the corresponding stochastic scenario where the deterministic Model III admits a periodic solution. By choosing $\Phi=0.8$ we obtain Figs. 9 and 10 where Fig. 9a shows that in the absence of random fluctuations, the task demand and work activity change periodically with the peaks/valleys of each cycle being equal. When random noise is introduced (Fig. 9b), the peaks/valleys of each cycle are different. This dynamics reflects the real data shown in Fig. 11 (working activity of a colony with 97 ants over 5 mins). Figure 10 also suggests that as the intensity of noise increases, the shape of the periodic solution becomes more and more disordered.



42 Page 28 of 53 T. Feng et al.

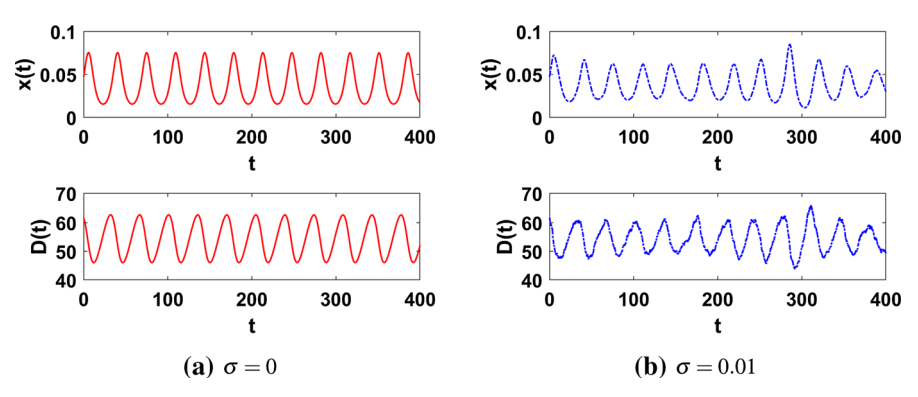


Fig. 9 Time series of Model (11) and Model III with $\Phi = 0.8$. The other parameters are given by $\theta = 5, b = 1.1, \delta_0 = 0.5, \gamma = 0.05, \delta = 0.7, \alpha = 0.005, N = 200, x(0) = 0.0473, D(0) = 61.63$

5.2 Case study: the working demand has a carrying capacity

The stochastic version of Model IV is given by:

$$dx(t) = x \left[\frac{\frac{D}{\theta}}{\frac{Dx}{\theta} + \Phi N^{\delta_0} (1 - x)} - 1 \right] dt,$$

$$dD(t) = \left[\gamma N^{\delta} \left(1 - \frac{D}{KN^{\delta}} \right) - \alpha N x D \right] dt + \sigma D(t) dB(t).$$
(12)

The previous subsection has shown that the size of $\delta - \delta_0 - 1$ does not affect the way the noise affects the work activity and the task command. In the remaining, we only show the numerical results of case $\delta - \delta_0 - 1 < 0$. By Theorem 2, the dynamics of Model IV can be summarized as:

- (a) If $\Phi < 0.1238$, Model IV has two equilibria: the working-free equilibrium $E_0^* = (x_0^*, D_0^*) = (0, 40.8057)$ being unstable and the resting-free equilibrium $E_1^* = (x_1^*, D_1^*) = (1, 3.7096)$ being globally asymptotically stable.
- (b) If $0.1238 < \Phi < 1.3615$, Model IV has three equilibria: the working-free equilibrium E_0^* and the resting-free equilibrium E_1^* being unstable and

$$\hat{E}^* = (\hat{x}^*, \hat{D}^*) = \left(\frac{4.9013 - 3.6\Phi}{36\Phi}, 29.9719\Phi\right)$$

being globally asymptotically stable.

(c) If $\Phi > 1.3615$, Model IV has two equilibria: E_0^* being globally asymptotically stable and E_1^* being unstable.

In the following, we study how random fluctuations affect task demand and work activity in scenarios (a), (b), and (c), respectively. By choosing $\Phi = 0.1$ and $\Phi = 1.3$, we explore the effects of random fluctuations on task demand and work activity in



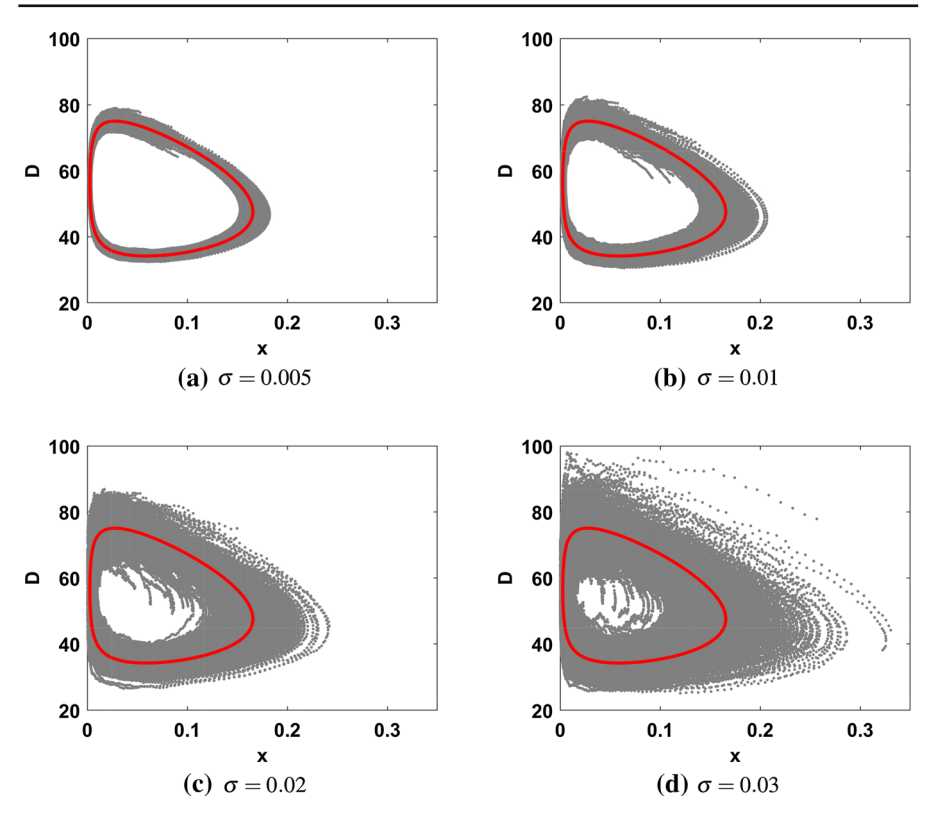


Fig. 10 Phase diagrams of solutions of Model (11) and Model III under 500 replicates in one cycle. The parameters are given by $\Phi = 0.8$, $\theta = 5$, b = 1.1, $\delta_0 = 0.5$, $\gamma = 0.05$, $\delta = 0.7$, $\alpha = 0.005$, N = 200, x(0) = 0.0449, D(0) = 74.281. The red lines and gray dots denote the solutions of the Model III and the stochastic Model (11), respectively

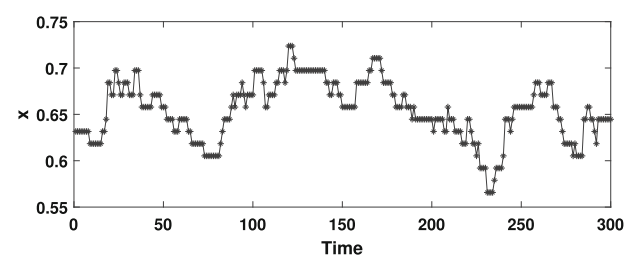


Fig. 11 Time series diagram (in seconds) of working activity of a colony with 97 ants. The colony was collected from the field in June 2014 and house in an artificial observation nest in the lab. The data was collected from a 5 min video recorded between noon and 5pm on June 28, 2014



42 Page 30 of 53 T. Feng et al.

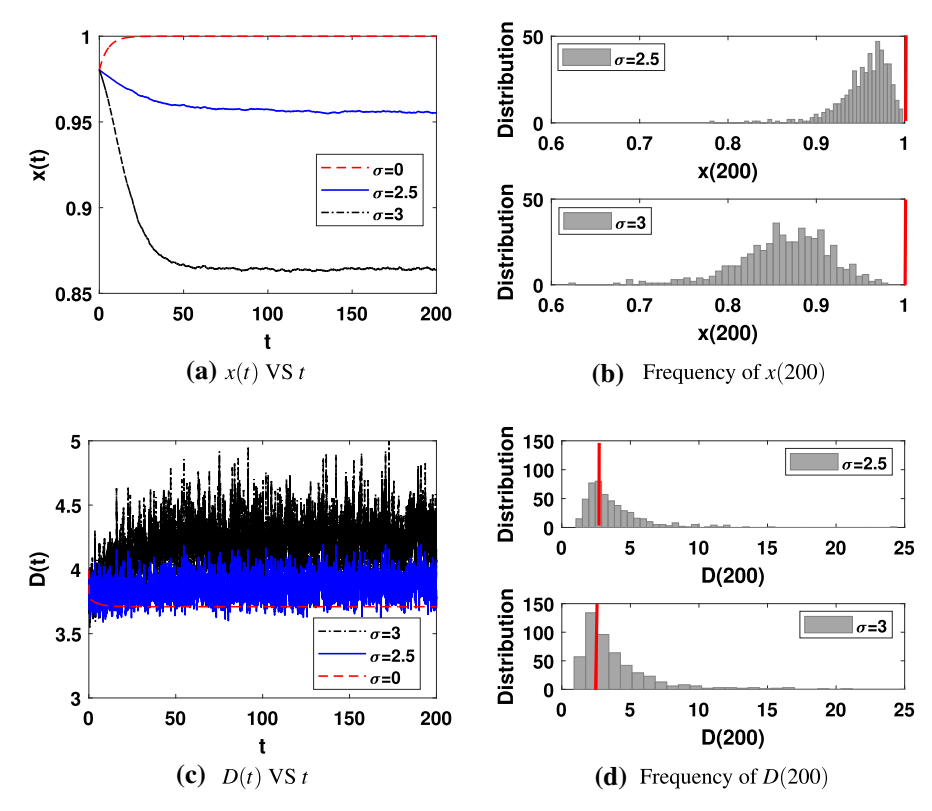


Fig. 12 Empirical mean and frequency of Model (12) and Model IV with $\Phi=0.1$ over 500 trajectories. The other parameters are given by $\theta=3.6$, K=1, $\delta_0=0.4$, $\gamma=1$, $\delta=0.7$, $\alpha=0.05$, N=200, x(0)=0.99, D(0)=4. Red lines indicate the solution of Model IV, blue and black lines indicate the empirical mean of the stochastic solution with $\sigma=2.5$ and 3. Figure 12b, d are frequency of the stochastic model at time t=200

scenarios (a) and (b), respectively (see Figs. 12 and 13). We find that the effects of random fluctuations in these two scenarios are consistent with the effects of random fluctuations in scenarios (a) and (b) of Model III (see Sect. 5.1): although random fluctuation generates an increase in average for task demand D, the working activity x of the colony decreases in average over 500 replicates.

Now, we study the scenario (c) by choosing $\Phi = 3$. The simulations are shown in Fig. 14. Figure 14a indicates that the work activity x(t) in Model (12) and Model IV tends to zero, and the higher the intensity of noise, the later the solution tends to 0. This result suggests that although random fluctuations cannot prevent the tendency to rest at all times but have delay effects. Figure 14b shows that the stochastic solution D(t) fluctuates around the solution of Model IV, and the amplitude of fluctuation is positively related to the intensity of noise.

Our study of stochastic versions of Model III and IV provides us the following insights:



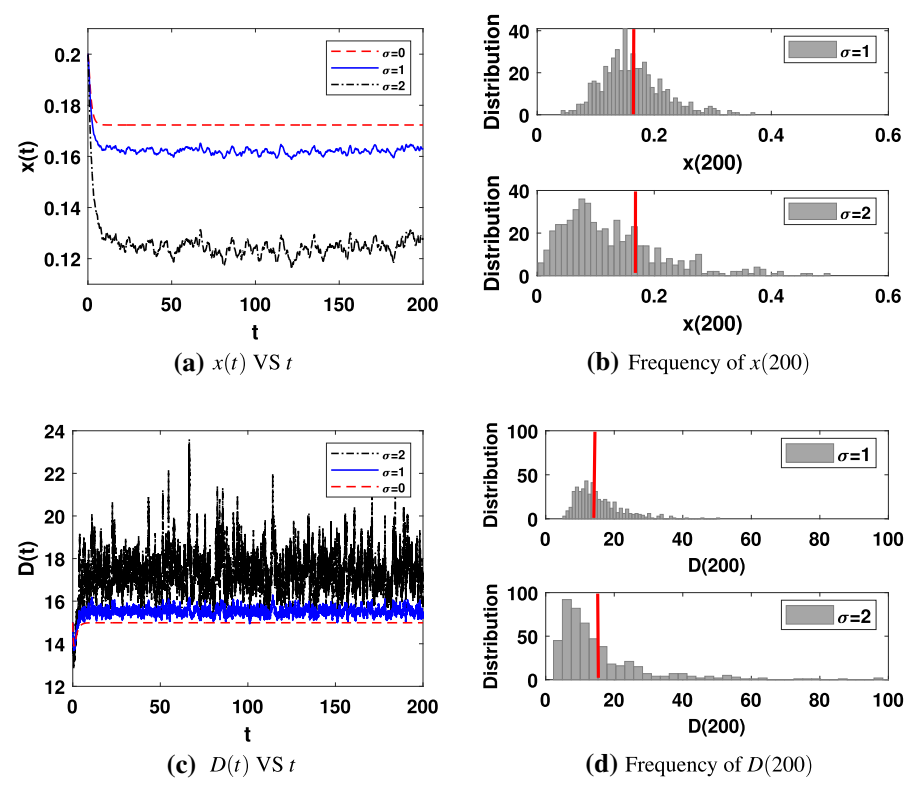


Fig. 13 Empirical mean and frequency of Model (12) and Model IV with $\Phi = 1.3$ over 500 trajectories. The other parameters are given by $\theta = 3.6$, K = 1, $\delta_0 = 0.4$, $\gamma = 1$, $\delta = 0.7$, $\alpha = 0.05$, N = 200, x(0) = 0.2, D(0) = 12. Red lines indicate the solution of Model IV, blue and black lines indicate the empirical mean of the stochastic solution with $\sigma = 1$ and 2. Fig. 13b, d are frequency of the stochastic model at time t = 200

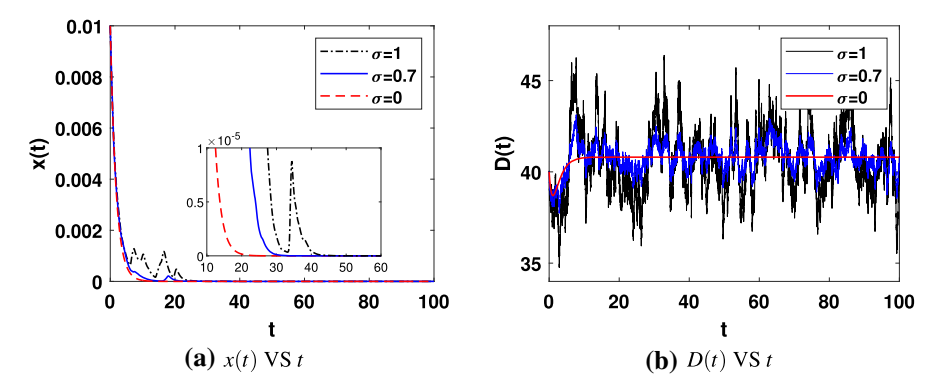


Fig. 14 Empirical mean of Model (12) and Model IV with $\Phi = 3$ over 500 trajectories. The other parameters are given by $\theta = 3.6$, K = 1, $\delta_0 = 0.4$, $\gamma = 1$, $\delta = 0.7$, $\alpha = 0.05$, N = 200, x(0) = 0.01, D(0) = 40



42 Page 32 of 53 T. Feng et al.

1. Noise can increase task demand and decrease the levels of working activity in average (i) By comparing to the dynamics of the the deterministic Model III or Model IV in three scenarios, the empirical mean of working activity *x* in the stochastic system (11) is almost certainly lower than its ODE model (see Figs. 7a, 8a, 12a and 13a), while the empirical mean of task demand *D* in the stochastic system (11) is almost certainly higher (see Figs. 7c, 8c, 12c, 13c). (ii) When the colony in Model IV spends all the time on resting, random fluctuations cannot change the colony being rest all the time but have delay effects (see Fig. 14a).

- 2. Effects of noise with different intensities The amplitude of the fluctuating solution for stochastic models is positively correlated with the intensity of the noise (see Figs. 7, 8, 9, 10, 11, 12, 13, 14). In addition, as the intensity of noise increases, the variance of the frequency (over 500 replicates) of stochastic solutions becomes larger. This suggests that large noise may lead to richer dynamics of the colony.
- 3. *The existence of stationary distribution* According to previous research experience (Cai et al. 2015; Feng et al. 2019), Figs. 7, 8, 12 and 13 suggest that there appears to be a stationary distribution of the stochastic system. This could be our future work to prove the existence of this stationary distribution even though it is challenging.
- 4. Random fluctuations can explain almost-cyclic dynamics observed in experiments Please see the experimental data in Fig. 11 and the simulation of Fig. 9b as an example for comparison.

6 Conclusion

In this paper, we have formulated a general dynamical compartmental model to explore the underlying mechanisms of task allocation in social insect colonies at the colony level. Our proposed deterministic model incorporates both internal factors (e.g., the varied thresholds for different tasks) and external factors (e.g., task demands/stimulus from the environment). The proposed model is also suitable for measuring the effects of nonlinear metabolic scaling on task allocation and rest probability, which in turn plays a role in improving our understanding of the dynamics of complex biological systems. This work is a nice extension of a mathematical framework introduced by Kang and Theraulaz 2016 that study how colony size and social communication affect the task allocation and division of labor.

Our theoretical results and the related biological implications provide us some answers to the three questions proposed in the Introduction: (i) how the metabolic scaling affects the task allocation and resting probability of social insect colonies, as colony size increases? (ii) how colony size affects the working activity in different scenarios of working versus resting? (iii) how the random fluctuation affects the working activity and task demand of social insect colonies?

We first explored the scaling effects of colony size on the resting probability. The theoretical result (Sect. 3.1) suggests that the colony size can affect the likelihood of resting in several ways: (a) when the nonlinear metabolic scaling of all tasks is large enough (i.e., larger than the nonlinear metabolic scaling of resting + 1), increasing the colony size can decrease the probability of resting; (b) when the nonlinear metabolic scaling of all tasks is small enough (i.e., smaller than the nonlinear metabolic scaling



of resting + 1), increasing the colony size can increase the probability of resting; (c) when there are two tasks (namely the inside colony task and the outside colony task), if the nonlinear metabolic scaling of the inside colony task and the outside colony task is small and large enough, respectively (i.e., smaller and larger than the nonlinear metabolic scaling of resting + 1, respectively), the relationship between the colony size and the resting probability depending on whether the colony is mature or not: if the colony is immature, increasing the colony size can increase the probability of resting. Otherwise, increasing the colony size can decrease the probability of resting.

These theoretical outputs are supported by experimental evidence. Indeed, empirical studies show that increasing group size can either increase or decrease the proportion of inactive workers in the group. For example, in the ant *Aphaenogaster senilis*, the amount of work performed by workers is highly correlated with the number of workers: the proportion of inactive individuals increases from 33% to 55% when the number of workers increases from 50 to 200 (Ruel et al. 2012), while in the social spider *Mallos gregalis*, larger colonies usually have a lower proportion of inactive workers (Tietjen 1986). Broadly, these different relationships between group size and inactivity can be explained by context-specific differences in how group size affects overall efficiency. As discussed in Sect. 3.11, larger groups may be more efficient which should lead to a higher proportion of inactive workers as they have more opportunities to rest (Jeanson et al. 2007), or large groups may have more overhead costs and thus the colony must work more to meet its needs resulting in fewer inactive workers.

Highly inactive workers are found among all taxa of social insects, typically making up more than 50% of the colonies (Charbonneau et al. 2017a). Inactivity has been shown to decrease with worker age in two distantly related species of ants with different life histories, suggesting that the broad pattern of worker inactivity among social insect taxa may result from age-related constraints (e.g., inexperience or still developping neurophysiologies)(D. Charbonneau, unpublished results). However, in addition to age-related constraints, inactive workers have been shown to play additional roles and sometimes provide benefits to the colony. Perhaps one of the most commonly suggested functions of inactive workers is acting as a pool of reserve labor that allows colonies to buffer against short term changes in demand or available workforce. This function has been both rejected in some species/contexts

(Fewell and Winston 1992; Jandt et al. 2012; O'Donnell 1998; Gardner et al. 2007; Johnson 2002)(reviewed in Charbonneau and Dornhaus 2015a, Charbonneau et al. 2017a), and supported in others (Charbonneau et al. 2017b; Hasegawa et al. 2016), suggesting that inactive workers may only act as 'reserves' in specific contexts. Our theoretical results suggest that perhaps inactives may only act as 'reserves' in species that can afford to have them (i.e., colonies of sufficient size, whose efficiency increases with colony size), while colonies whose overhead increases with colony size may not be able to utilize the already present (due to their young age) inactive workers.

When multiple tasks appear in the colony, the situation can become very complicated. For the sake of simplicity, we focused on the scenario with two task groups (i.e., the inside colony task and the outside colony task) to illustrate how the nonlinear metabolic scaling affects the task allocation, as colony increases. The theoretical results (Sect. 3.2) support that: when the relative stimulus of resting is constant and lower than the relative stimulus of working, increasing the colony size can increase



42 Page 34 of 53 T. Feng et al.

the allocation of the task group with larger nonlinear metabolic scaling and decrease the allocation of the task group with smaller nonlinear metabolic scaling; when the relative stimulus of resting is constant and higher than the relative stimulus of working: (i) if the nonlinear metabolic scaling of both task groups is large (resp. small) enough, increasing the colony size can increase (resp. decrease) the allocation of all task groups and decrease (resp. increase) the allocation of resting; (ii) if the nonlinear metabolic scaling of the inside and out task groups is large enough and small enough respectively, the increase of colony size can increase (resp. decrease) the allocation of the task group with larger (resp. smaller) nonlinear metabolic scaling, and the allocation of resting depends on the maturity of the colony; when the relative stimulus of resting is an increasing function of the working effort, there are several ways in which the nonlinear metabolic scaling can affect the allocation of tasks and resting, depending on the maturity and colony size.

Generally, larger decentralized groups are expected to have more specialized individuals and increasingly sophisticated mechanisms for allocating tasks (e.g., cellular differentiation in multicellular organisms). As such social insects have long been theorized to follow similar trends of larger colonies to have more complex division of labor (Oster and Wilson 1978), however, empirical data has yet to satisfactorily show this (Dornhaus et al. 2012). Furthermore, we often assume that greater specialization leads to increased efficiency, but that is not necessarily the case. Indeed, increased specialization, such as via morphologically specialized workers, often leads to decreased flexibility (Charbonneau and Dornhaus 2015a). For example, colonies of *Pogonomyrmex badius* ants were unable to compensate for the loss of half of their foragers from experimental removal and consequently lost half of their brood as a result (Kwapich and Tschinkel 2013). Thus, the effects of group size on collective behaviors are again entirely context specific. Our theoretical outputs follow a similar trend where the effects of group size on task allocation, and on the proportion of inactive workers is dependent on the relative increase in efficiency as colony size increases.

We applied our general model to study the dynamics of the working effort versus resting at four different scenarios, namely: (i) The resting demand is a constant function depending on the colony size. (ii) The resting demand is an increasing function of the working effort. (iii) The working demand has an enhanced response threshold. (iv) The working demand has a carrying capacity. Our theoretical result (Theorem 2) shows that:

- 1. Cases (i) and (ii) have similar dynamics (Figs. 1, 2): if the resting demand is small enough, the colony works all the time, while if the resting demand is large enough, the colony rests in equilibrium patterns (i.e., the ratio of resting workers remains at a certain level). One difference between cases (i) and (ii) is that when the resting command is large enough, case (i) has a lower probability of resting than case (ii) under the same conditions (i.e., all parameters are the same).
- 2. When the working demand has a carrying capacity (i.e., case (iv), see Fig. 3): if the resting demand is small enough, the colony works all the time; if the resting demand is moderate, the colony rests in equilibrium patterns; if the resting demand is large enough, the colony rests all the time. Case (iv) differs from cases (i)-(ii) in that if the resting command is large enough, the colony may rest all the time,



- indicating that the colony may rest all the time if the working demand has a limited carrying capacity.
- 3. The dynamics of the case (iii) is more complicated than the other three cases (Fig. 4). When the resting demand is small enough, the colony works all the time. When the resting demand is large enough, the colony may rest in varied patterns, i.e., the ratio of resting workers either remains at a certain level or changes at a fixed cycle. When the enhanced response threshold constant is 0, case (iii) is exactly the same as the case (i), indicating that an enhanced response threshold can lead to the cycle dynamics. Specifically, the solution of the case (iii) can go through two supercritical Hopf bifurcations successively with varying the level of the enhanced response threshold (Fig. 6): when the solution crosses through the first Hopf bifurcation from the left, a stable periodic solution appears, and the amplitude of the periodic solution increases first and then decreases with the enhanced response threshold increases; when the solution crosses through the second Hopf bifurcation from the left, the periodic solution disappears. Since the change of the amplitude of the periodic solution looks like a bubble, it is called the bubble phenomenon, which was once found in the SIS disease models with time delay and media/awareness effects (Liu et al. 2015), but this is the first time we found bubble phenomenon in task allocation of social insect colonies. It reveals the dynamic process of the generation and disappearance of periodic orbits in social insect colonies with varying the level of enhanced response threshold. Similarly, the results show that the colony size can also cause bubble phenomenon (Fig. 6).

Like other biological systems, interactions between social insect colonies and the environment are noisy (Costello and Symes 2014; Barton et al. 2018; Lee et al. 2012). In social insect colonies, the task allocation of workers comes from responses to task stimuli/needs, and the process of workers receiving stimuli may be affected by environmental noise (i.e., Couzin and Franks 2003). This can be explained by, for example, random fluctuations affecting the accuracy of information exchange among workers (by affecting the pheromones or the antennae sounds), thereby affecting the task stimulus/task demands. To peek into the effects of random fluctuations on the dynamics of task allocation, we assumed that the intensity of environmental noise is proportional to the size of the task demand, and derived two white noise-driven stochastic models based on cases (iii) and (iv). For each case, we focused on the effects of random fluctuations on task allocation under three different dynamic situations (Sects. 5.1 and 5.2). Numerical simulation results of the stochastic models indicate that: (1) Noise can regulate task demand and work activity in the following ways: when the colony rests at a certain level, the intervention of random fluctuations makes the average of the task demand (over 500 replicates) higher, and the average of the resting level becomes lower; when the colony spends all the time on resting, random fluctuations can not change the colony being rest all the time but have delay effects; when the task demand and the resting level change periodically, the intervention of random fluctuations can make the periodicity irregular. (2) Increased noise intensity may lead to more possibilities for the system. (3) Noise may explain the volatility of experimental data (see Fig. 11).



42 Page 36 of 53 T. Feng et al.

Our paper provides a new modeling and theoretical framework for studying task allocation of social insect colonies. Our theoretical results provide important biological insights into how the scaling effects of colony size affects task allocation and resting probability. Besides, four application scenarios based on the actual situation are presented on the level of working activity and resting. The effects of random fluctuations on task stimuli are also included in the study of task allocation of social insect colonies. Despite these promising results above, some important factors are needed to address further. For example, (l) our framework only considers the dynamics of the colony without space. However, the task groups and demands are unevenly distributed in space. It would be interesting to take into account the effects of spatial scale on the task allocation of social insect colonies; and (2) To fully understand the task allocation of social insect colonies, experimental data should be introduced and combined with theoretical results to obtain a better understanding of the task allocation of social insect colonies. Those two points are our ongoing work.

7 Proofs

7.1 Proof of Theorem 1

Proof Since $\sum_{i=0}^{m} x_i(0) = 1$ and $\sum_{i=0}^{m} x_i' = 0$, we can conclude that

$$\sum_{i=0}^{m} x_i(t) = 1 \text{ and } 0 \le x_i(t) \le 1 \text{ for all } t \ge 0.$$

For any initial condition taken in Ω , we have follows:

$$\frac{dx_i}{dt}\Big|_{x_i=0} = 0, \ \frac{dD_i}{dt}\Big|_{D_i=0} = \gamma_i N^{\delta_i} > 0, i = 1, \dots, m,$$

which implies that the Model (1) is positively invariant in Ω according to Theorem A.4 (p.423) in Thieme (2003).

Notice that N is strictly positive, and

$$D_i' = \gamma_i N^{\delta_i} \left[1 - \frac{x_i D_i}{\theta_i \hat{D}_i} \right] \ge \gamma_i N^{\delta_i} \left[1 - \frac{D_i}{\theta_i \hat{D}_i} \right],$$

we have

$$\liminf_{t\to\infty} D_i(t) \ge \theta_i \hat{D}_i = \frac{\gamma_i N^{\delta_i-1}}{\alpha_i}.$$

Assume that $X^* = [x_0^*, x_1^*, ..., x_m^*]$ and $D^* = [D_1^*, D_2^*, ..., D_m^*]$ is an equilibrium of Model (1). If $\frac{D_0}{\theta_0} = \Phi N^{\delta_0}$, we have the following equations hold for $i \ge 1$:

$$1 - \frac{x_i^* D_i^*}{\theta_i \hat{D}_i} = 0 \Rightarrow \frac{x_i^* D_i^*}{\theta_i} = \hat{D}_i,$$



$$\begin{split} \frac{\frac{D_{i}^{*}}{\theta_{i}}}{\sum_{k=0}^{m} \frac{D_{k}^{*} x_{k}^{*}}{\theta_{k}}} - 1 &= 0 \Rightarrow \frac{D_{i}^{*}}{\theta_{i}} = \sum_{k=0}^{m} \frac{D_{k}^{*} x_{k}^{*}}{\theta_{k}} = \sum_{k=1}^{m} \hat{D}_{k} \\ &+ \Phi N^{\delta_{0}} x_{0}^{*} = \hat{D} + \Phi N^{\delta_{0}} x_{0}^{*}, \end{split}$$

and for i = 0, we have

$$\frac{\frac{D_0}{\theta_0}}{\sum_{k=1}^{m} \frac{D_k^* x_k^*}{\theta_k} + \frac{D_0 x_0^*}{\theta_0}} = 1 \Rightarrow \Phi N^{\delta_0} = \hat{D} + \Phi N^{\delta_0} x_0^*$$
$$\Rightarrow x_0^* = 1 - \frac{\hat{D}}{\Phi N^{\delta_0}} \text{ if } \Phi N^{\delta_0} > \hat{D}$$

and

$$x_0^* = 0 \text{ if } \Phi N^{\delta_0} < \hat{D}.$$

Therefore, if $\Phi N^{\delta_0} > \hat{D}$, we have

$$x_0^* = 1 - \frac{\hat{D}}{\Phi N^{\delta_0}}, \ D_i^* = \theta_i \left(\hat{D} + \Phi N^{\delta_0} x_0^* \right) = \theta_i \Phi N^{\delta_0}$$

and

$$x_i^* = \frac{\hat{D}_i \theta_i}{D_i^*} = \frac{\hat{D}_i}{\Phi N^{\delta_0}}$$
 for all $1 \le i \le m$.

If $\Phi N^{\delta_0} < \hat{D}$, we have

$$x_0^* = 0$$
, $D_i^* = \theta_i \left(\hat{D} + \Phi N^{\delta_0} x_0^* \right) = \theta_i \hat{D}$ and $x_i^* = \frac{\hat{D}_i \theta_i}{D_i^*} = \frac{\hat{D}_i}{\hat{D}}$ for all $1 \le i \le m$.

If $\frac{D_0}{\theta_0} = wN^{\delta_0}(1-x_0)$, we have the following equations hold for $i \ge 1$:

$$1 - \frac{x_i^* D_i^*}{\theta_i \hat{D}_i} = 0 \Rightarrow \frac{x_i^* D_i^*}{\theta_i} = \hat{D}_i,$$

$$\frac{\frac{D_i^*}{\theta_i}}{\sum_{k=0}^m \frac{D_k^* x_k^*}{\theta_k}} - 1 = 0 \Rightarrow \frac{D_i^*}{\theta_i} = \sum_{k=0}^m \frac{D_k^* x_k^*}{\theta_k} = \sum_{k=1}^m \hat{D}_k + w N^{\delta_0} x_0^* (1 - x_0^*)$$

$$= \hat{D} + w N^{\delta_0} (1 - x_0^*) x_0^*,$$



42 Page 38 of 53 T. Feng et al.

and for i = 0, we have

$$\frac{\frac{D_0}{\theta_0}}{\sum_{k=1}^{m} \frac{D_k^* x_k^*}{\theta_k} + \frac{D_0 x_0^*}{\theta_0}} = 1 \Rightarrow w N^{\delta_0} (1 - x_0^*) = \hat{D} + w N^{\delta_0} (1 - x_0^*) x_0^*$$
$$\Rightarrow x_0^* = 1 - \sqrt{\frac{\hat{D}}{w N^{\delta_0}}} \text{ if } w N^{\delta_0} > \hat{D}$$

and

$$x_0^* = 0 \text{ if } w N^{\delta_0} < \hat{D}.$$

Therefore, if $wN^{\delta_0} > \hat{D}$, we have

$$x_0^* = 1 - \sqrt{\frac{\hat{D}}{wN^{\delta_0}}}, \ D_i^* = \theta_i \left(\hat{D} + wN^{\delta_0}(1 - x_0^*)x_0^*\right) = \theta_i \sqrt{\hat{D}wN^{\delta_0}}$$

and

$$x_i^* = \frac{\hat{D}_i \theta_i}{D_i^*} = \frac{\hat{D}_i}{\sqrt{\hat{D}wN^{\delta_0}}} \text{ for all } 1 \le i \le m.$$

If $wN^{\delta_0} < \hat{D}$, we have

$$x_0^* = 0, \ D_i^* = \theta_i \left(\hat{D} + w N^{\delta_0} (1 - x_0^*) x_0^* \right) = \theta_i \hat{D}$$

and

$$x_i^* = \frac{\hat{D}_i \theta_i}{D_i^*} = \frac{\hat{D}_i}{\hat{D}}$$
 for all $1 \le i \le m$.

Let $v_{0i} = \frac{x_0}{x_i}$ and $v_{i0} = \frac{x_i}{x_0}$, then we have

$$v'_{0i} = \frac{x'_0}{x_i} - \frac{x_0 x'_i}{x_i^2} = v_{0i} \frac{\frac{D_0}{\theta_0} - \frac{D_i}{\theta_i}}{\sum_{k=0}^m \frac{D_k x_k}{\theta_k}},$$

$$v'_{i0} = \frac{x'_i}{x_0} - \frac{x_i x'_0}{x_0^2} = v_{i0} \frac{\frac{D_i}{\theta_i} - \frac{D_0}{\theta_0}}{\sum_{k=0}^m \frac{D_k x_k}{\theta_k}}.$$

Since $\liminf_{t\to\infty} D_i(t) \ge \theta_i \hat{D}_i$, we have follows:



1. If $\frac{D_0}{\theta_0} = \Phi N^{\delta_0} < \hat{D}_i$, the following inequalities hold

$$v'_{0i} = v_{0i} \frac{\frac{D_0}{\theta_0} - \frac{D_i}{\theta_i}}{\sum_{k=0}^{m} \frac{D_k x_k}{\theta_k}} \le v_{0i} \frac{\Phi N^{\delta_0} - \hat{D}_i}{\sum_{k=0}^{m} \frac{D_k x_k}{\theta_k}} < 0,$$

$$v_{i0}' = v_{i0} \frac{\frac{D_i}{\theta_i} - \frac{D_0}{\theta_0}}{\sum_{k=0}^{m} \frac{D_k x_k}{\theta_k}} \ge v_{i0} \frac{\hat{D}_i - \Phi N^{\delta_0}}{\sum_{k=0}^{m} \frac{D_k x_k}{\theta_k}} > 0,$$

which imply that

$$\limsup_{t \to \infty} v_{0i}(t) = \limsup_{t \to \infty} \frac{x_0(t)}{x_i(t)} = 0 \text{ and } \limsup_{t \to \infty} v_{i0}(t) = \limsup_{t \to \infty} \frac{x_i(t)}{x_0(t)} = \infty.$$

2. If $\frac{D_0}{\theta_0} = w N^{\delta_0} (1 - x_0)$ and $w N^{\delta_0} < \hat{D}_i$, the following inequalities hold

$$\begin{split} v_{0i}' &= v_{0i} \frac{\frac{D_0}{\theta_0} - \frac{D_i}{\theta_i}}{\sum_{k=0}^{m} \frac{D_k x_k}{\theta_k}} \leq v_{0i} \frac{w N^{\delta_0} (1 - x_0) - \hat{D}_i}{\sum_{k=0}^{m} \frac{D_k x_k}{\theta_k}} \leq v_{0i} \frac{w N^{\delta_0} - \hat{D}_i}{\sum_{k=0}^{m} \frac{D_k x_k}{\theta_k}} < 0, \\ v_{i0}' &= v_{i0} \frac{\frac{D_i}{\theta_i} - \frac{D_0}{\theta_0}}{\sum_{k=0}^{m} \frac{D_k x_k}{\theta_k}} \geq v_{i0} \frac{\hat{D}_i - w N^{\delta_0} (1 - x_0)}{\sum_{k=0}^{m} \frac{D_k x_k}{\theta_k}} > 0, \end{split}$$

which imply that

$$\limsup_{t \to \infty} v_{0i}(t) = \limsup_{t \to \infty} \frac{x_0(t)}{x_i(t)} = 0 \text{ and } \limsup_{t \to \infty} v_{i0}(t) = \limsup_{t \to \infty} \frac{x_i(t)}{x_0(t)} = \infty.$$

Therefore, if there exists an i such that $wN^{\delta_0} < \hat{D}_i$ for $\frac{D_0}{\theta_0} = wN^{\delta_0}(1-x_0)$ or $\frac{D_0}{\theta_0} = \Phi N^{\delta_0} < \hat{D}_i$ holds, we have

$$\lim_{t \to \infty} x_0(t) = 0.$$

7.2 Proof of Theorem 2

Proof The proof of the existence of equilibria is straightforward, so it is omitted here. To prove the stability of equilibria, let E^* be the corresponding equilibrium of the above four systems, $J|_{(E^*)}$ the corresponding Jacobian matrix evaluated at E^* and $\lambda_i(E^*)(i=1,2)$ the eigenvalues of $J|_{(E^*)}$.

Model I The system (7) always has an equilibrium E^* . The Jacobian matrix of System (7) evaluated at E^* is

$$J|_{(E^*)} = \begin{pmatrix} \frac{\Phi\theta\alpha N^{\delta_0+1-\delta}}{\gamma} - 1 & 0 \\ -\gamma N^{\delta} & -\alpha N \end{pmatrix}.$$



42 Page 40 of 53 T. Feng et al.

Direct computation yields

$$\lambda_1(E^*) = -\alpha N < 0 \text{ and } \lambda_2(E^*) = \frac{\alpha \theta N^{\delta_0 + 1 - \delta}}{\gamma} \left(\Phi - \frac{\gamma N^{\delta - \delta_0 - 1}}{\alpha \theta} \right).$$

It follows that E^* is locally asymptotically stable if $\Phi < \frac{\gamma N^{\delta-\delta_0-1}}{\alpha \theta}$, and it is unstable if $\Phi > \frac{\gamma N^{\delta-\delta_0-1}}{\alpha \theta}$.

Case (1) $\Phi < \frac{\gamma N^{\delta-\delta_0-1}}{\alpha \theta}$. In this case, E^* is the unique equilibrium of System (7). The Pioncare-Bendixson theorem (Hale 1980) implies that all solutions of System (7) converge to the equilibrium E^* , i.e., E^* is globally asymptotically stable.

Case (2) $\Phi > \frac{\gamma N^{\delta - \delta_0 - 1}}{\alpha \theta}$. In this case, E^* is unstable and System (7) has a unique interior equilibrium $\hat{E}^*(\hat{x}^*, \hat{D}^*)$. The Jacobian matrix of System (7) evaluated at \hat{E}^* is

$$J|_{(\hat{E}^*)} = \begin{pmatrix} 0 & \frac{\sigma\theta N^{\delta_0}\hat{x}^*(1-\hat{x}^*)}{\left[\hat{D}^*\hat{x}^* + \sigma\theta N^{\delta_0}(1-\hat{x}^*)\right]^2} \\ -\alpha N\hat{D}^* & -\alpha N\hat{x}^* \end{pmatrix}.$$

Then we have

$$\lambda_1(\hat{E}^*) + \lambda_2(\hat{E}^*) = -\alpha N \hat{x}^* < 0$$

and

$$\lambda_1(\hat{E}^*)\lambda_2(\hat{E}^*) = \frac{\alpha \hat{D}^* \Phi \theta N^{\delta_0 + 1} \hat{x}^*}{\left[\hat{D}^* \hat{x}^* + \Phi \theta N^{\delta_0} (1 - \hat{x}^*)\right]^2} (1 - \hat{x}^*) > 0,$$

which indicates that $\lambda_1(\hat{E}^*) < 0$, $\lambda_2(\hat{E}^*) < 0$. Thus the equilibrium \hat{E}^* is locally asymptotically stable. To show the global stability of \hat{E}^* , we only need to rule out the existence of periodic orbit for the System (7). Suppose that $\Gamma(t) = (x(t), D(t))$ is an arbitrary nontrivial periodic orbit of the System (7) with the least period T > 0, and J(x(t), D(t)) is the Jacobian matrix of System (7) around the periodic solution (x(t), D(t)). Let

$$\begin{split} \Delta(\Gamma(t)) &:= \int_0^T \operatorname{Trac}(J(x(t),D(t))) dt \\ &= \int_0^T \left(\frac{\frac{D(t)}{\theta} \Phi N^{\delta_0}}{\left[\frac{D(t)x(t)}{\theta} + \Phi N^{\delta_0} (1-x(t))\right]^2} - 1 - \alpha N x(t) \right) dt. \end{split}$$



Since

$$x' = x \left[\frac{\frac{D}{\theta}}{\frac{Dx}{\theta} + \Phi N^{\delta_0} (1 - x)} - 1 \right],$$

we have

$$\begin{split} &\frac{\frac{D}{\theta}\Phi N^{\delta_0}}{\left[\frac{Dx}{\theta} + \Phi N^{\delta_0}(1-x)\right]^2} \\ &= \left(\frac{x'}{x} + 1\right)^2 \frac{\theta \Phi N^{\delta_0}}{D} = \frac{x'}{x} + 1 - \frac{{x'}^2}{x(1-x)} - \frac{x'}{1-x}. \end{split}$$

It follows that

$$\Delta(\Gamma(t)) = \int_0^T \left(\frac{x'(t)}{x(t)} - \frac{x'(t)^2}{x(t)(1 - x(t))} - \frac{x'(t)}{1 - x(t)} - \alpha N x(t) \right) dt$$

$$= \int_0^T \left(\frac{x'(t)}{x(t)} - \frac{x'(t)}{1 - x(t)} \right) dt$$

$$+ \int_0^T \left(-\frac{x'(t)^2}{x(t)(1 - x(t))} - \alpha N x(t) \right) dt$$

$$< 0.$$

By the divergency criterion (Hale 1980), all the periodic solutions should be orbitally stable. This contradicts the local stability of the equilibrium \hat{E}^* , i.e., \hat{E}^* is globally asymptotically stable.

Model II The System (8) always has an equilibrium E^* . The Jacobian matrix of the System (8) evaluated at E^* is

$$J|_{(E^*)} = \begin{pmatrix} \frac{\theta w \alpha N^{\delta_0 + 1 - \delta}}{\gamma} - 1 & 0 \\ -\gamma N^{\delta} & -\alpha N \end{pmatrix}.$$

By calculating the eigenvalues, we have

$$\lambda_1(E^*) = -\alpha N < 0, \ \lambda_2(E^*) = \frac{\alpha \theta N^{\delta_0 + 1 - \delta}}{\gamma} \left(w - \frac{\gamma N^{\delta - \delta_0 - 1}}{\alpha \theta} \right).$$

It follows that E^* is locally asymptotically stable if $w < \frac{\gamma N^{\delta - \delta_0 - 1}}{\alpha \theta}$, while it is unstable if $w > \frac{\gamma N^{\delta - \delta_0 - 1}}{\alpha \theta}$.



42 Page 42 of 53 T. Feng et al.

Case (1) $w < \frac{\gamma N^{\delta-\delta_0-1}}{\alpha\theta}$. In this case, E^* is the unique equilibrium of System (8). It then follows from the Pioncare-Bendixson theorem (Hale 1980) that all solutions of System (8) converge to the equilibrium E^* , i.e., E^* is globally asymptotically stable.

System (8) converge to the equilibrium E^* , i.e., E^* is globally asymptotically stable. Case (2) $w > \frac{\gamma N^{\delta-\delta_0-1}}{\alpha\theta}$. In this case, E^* is unstable and System (8) has a unique interior equilibrium $\hat{E}^*(\hat{x}^*, \hat{D}^*)$. The Jacobian matrix of System (8) evaluated at \hat{E}^* is

$$J|_{(\hat{E}^*)} = \begin{pmatrix} \frac{\theta\omega N^{\delta_0}\hat{x}^{*2}}{\hat{D}^*} - 1 & \frac{\theta\omega N^{\delta_0}\hat{x}^{*2}(1-\hat{x}^*)}{\hat{D}^{*2}} \\ -\alpha N\hat{D}^* & -\alpha N\hat{x}^* \end{pmatrix}.$$

Since

$$\frac{\theta \omega N^{\delta_0} \hat{x}^{*2}}{\hat{D}^*} = \sqrt{\frac{\gamma N^{\delta - \delta_0 - 1}}{\alpha \theta w}} = \hat{x}^* < 1,$$

we obtain that the eigenvalues $\lambda_1(\hat{E}^*)$, $\lambda_2(\hat{E}^*)$ satisfy

$$\lambda_1(\hat{E}^*) + \lambda_2(\hat{E}^*) = -\left(1 - \frac{\theta \omega N^{\delta_0} \hat{x}^{*2}}{\hat{x}^*} + \alpha N \hat{x}^*\right) < 0$$

and

$$\lambda_{1}(\hat{E}^{*})\lambda_{2}(\hat{E}^{*}) = \alpha N \hat{x}^{*} \left(1 - \frac{\theta \omega N^{\delta_{0}} \hat{E}^{*2}}{\hat{D}^{*}}\right) + \frac{\alpha \theta \omega N^{1+\delta_{0}} \hat{x}^{*2} (1 - \hat{x}^{*})}{\hat{D}^{*}} > 0,$$

which indicates that $\lambda_1(\hat{E}^*) < 0$, $\lambda_2(\hat{E}^*) < 0$. Thus the equilibrium \hat{E}^* is locally asymptotically stable. To further verify the global asymptotically stable of the equilibrium \hat{E}^* , we only need to rule out the existence of periodic orbit for the System (8). We assume that $\Gamma(t) = (x(t), D(t))$ is an arbitrary nontrivial periodic orbit of the System (8) with the least period T > 0, and J(x(t), D(t)) is the Jacobian matrix of System (8) around the periodic solution (x(t), D(t)). Let

$$\Delta(\Gamma(t)) := \int_0^T \operatorname{Trac}(J(x(t), D(t))) dt$$

$$= \int_0^T \left(\frac{\frac{D(t)}{\theta} w N^{\delta_0} x^2(t)}{\left[\frac{D(t)x(t)}{\theta} + w N^{\delta_0} x(t)(1 - x(t)) \right]^2} - 1 - \alpha N x(t) \right) dt.$$

Since

$$x' = x \left\lceil \frac{\frac{D}{\theta}}{\frac{Dx}{\theta} + wN^{\delta_0}x(1-x)} - 1 \right\rceil,$$



we have

$$\begin{split} &\frac{\frac{D}{\theta}wN^{\delta_0}x^2}{\left[\frac{Dx}{\theta}+wN^{\delta_0}x(1-x)\right]^2} = \left(\frac{x'}{x}+1\right)^2\frac{\theta wN^{\delta_0}x^2}{D} \\ &= \left(2-\frac{1}{1-x}\right)x'+x-\frac{{x'}^2}{1-x}. \end{split}$$

It follows that

$$\Delta(\Gamma(t)) = \int_0^T \left[\left(2 - \frac{1}{1 - x(t)} \right) x'(t) + x(t) - \frac{x'(t)^2}{1 - x(t)} - 1 - \alpha N x(t) \right] dt$$

$$= \int_0^T \left(2 - \frac{1}{1 - x(t)} \right) x'(t) dt$$

$$+ \int_0^T \left(-(1 - x(t)) - \frac{x'(t)^2}{1 - x(t)} - \alpha N x(t) \right) dt$$

$$< 0.$$

By the divergency criterion (Hale 1980), all the periodic solutions must be orbitally stable. This contradicts the local stability of the equilibrium \hat{E}^* , i.e., the equilibrium \hat{E}^* is globally asymptotically stable.

Model III The System (9) always has an equilibrium E^* . The Jacobian matrix of System (9) evaluated at E^* is

$$J|_{(E^*)} = \begin{pmatrix} \frac{\alpha\theta\Phi N^{\delta_0+1-\delta}}{\gamma(1+b)} - 1 & 0\\ -\gamma N^{\delta} & -\alpha N \end{pmatrix}.$$

By calculating the eigenvalues, we have

$$\lambda_1(E^*) = -\alpha N < 0, \ \lambda_2(E^*) = \frac{\alpha \theta N^{\delta_0 + 1 - \delta}}{\gamma(1+b)} \left(\Phi - \frac{\gamma(1+b)N^{\delta - \delta_0 - 1}}{\alpha \theta} \right).$$

Then E^* is locally asymptotically stable if $\Phi < \frac{\gamma(1+b)N^{\delta-\delta_0-1}}{\alpha\theta}$, and E^* is unstable if $\Phi > \frac{\gamma(1+b)N^{\delta-\delta_0-1}}{\alpha\theta}.$

Case (1) $\Phi < \frac{\gamma(1+b)N^{\delta-\delta_0-1}}{\alpha\theta}$. In this case, E^* is the unique equilibrium of System (9). It then follows from the Pioncare-Bendixson theorem (Hale 1980) that all solutions of System (9) converge to the equilibrium E^* , i.e., E^* is globally asymptotically stable.

Case (2) $\Phi > \frac{\gamma(1+b)N^{\delta-\delta_0-1}}{\alpha\theta}$. In this case, E^* is unstable and System (9) has an equilibrium $\hat{E}^*(\hat{x}^*, \hat{D}^*)$. The Jacobian matrix of System (9) evaluated at \hat{E}^* is

$$J|_{(\hat{E}^*)} = \begin{pmatrix} \frac{b\hat{x}^*(1-\hat{x}^*)}{1+b\hat{x}^*} & \frac{\hat{x}^*(1-\hat{x}^*)}{\hat{D}^*} \\ -\alpha N \hat{D}^* & -\alpha N \hat{x}^* \end{pmatrix}.$$



Page 44 of 53 T. Feng et al.

By computing the eigenvalues, we obtain that

$$\lambda_1(\hat{E}^*)\lambda_2(\hat{E}^*) = \alpha N\hat{x}^*(1-\hat{x}^*)\left(1-\frac{b\hat{x}^*}{1+b\hat{x}^*}\right) > 0$$

and

$$\lambda_1(\hat{E}^*) + \lambda_2(\hat{E}^*) = -\hat{x}^* \left(\alpha N - b + \frac{b(1+b)\gamma N^{\delta - \delta_0 - 1}}{\Phi \alpha \theta} \right).$$

Therefore, we can conclude that:

- When $b \alpha N \leq 0$ and $\Phi > \frac{\gamma(1+b)N^{\delta-\delta_0-1}}{\alpha^{\theta}}$, we have $\lambda_1(\hat{E}^*) + \lambda_2(\hat{E}^*) < 0$, i.e.,
- \hat{E}^* is locally asymptotically stable. When $b \alpha N > 0$ and $\frac{\gamma(1+b)N^{\delta-\delta_0-1}}{\alpha\theta} < \Phi < \frac{\gamma b(1+b)N^{\delta-\delta_0-1}}{\alpha\theta(b-\alpha N)} := \Phi^*$, we have $\lambda_1(\hat{E}^*) + \lambda_2(\hat{E}^*) < 0$, i.e., \hat{E}^* is locally asymptotically stable.
- When $b \alpha N > 0$ and $\Phi > \Phi^*$, we have $\lambda_1(\hat{E}^*) + \lambda_2(\hat{E}^*) > 0$, i.e., \hat{E}^* is unstable.

Notice that when $b > \alpha N$, the stability of \hat{E}^* is closely related to the parameter values. In the following, we apply local bifurcation theory to study the complex dynamics of \hat{E}^* when $b > \alpha N$.

We first choose Φ to be the bifurcation parameter. Let

$$f(\Phi) = (\alpha N - b)\Phi\alpha\theta + b(1+b)\gamma N^{\delta-\delta_0-1}.$$
 (13)

Since $f(\Phi^*) = 0$ and $f'(\Phi^*) < 0$, the equilibrium \hat{E}^* is locally asymptotically stable if $\Phi_0 < \Phi < \Phi^*$, while it is unstable if $\Phi > \Phi^*$. Then, by a similar argument (Qiu and Zhu 2016), we obtain that the system undergoes a Hopf bifurcation at $\Phi = \Phi^*$.

Since $\Phi > \frac{\gamma(1+b)N^{\delta-\delta_0-1}}{\alpha\theta} \Leftrightarrow b < \frac{\Phi\alpha\theta N^{\delta_0+1-\delta}}{\gamma} - 1 := b_0$, the system has an equilibrium \hat{E}^* if $b < b_0$. Next, we choose b to be the bifurcation parameter. By (13) we have

$$f(b) = \gamma N^{\delta - \delta_0 - 1} b^2 + \left(\gamma N^{\delta - \delta_0 - 1} - \Phi \alpha \theta \right) b + \alpha^2 N \Phi \theta.$$

Let

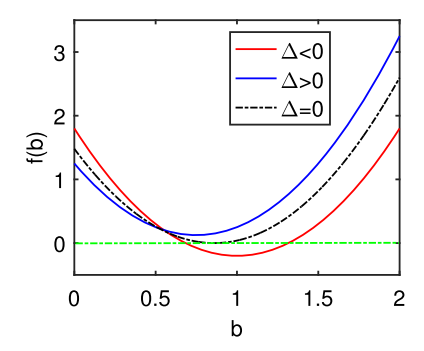
$$\Delta = \left(\gamma N^{\delta - \delta_0 - 1} - \Phi \alpha \theta\right)^2 - 4\gamma \alpha^2 \Phi \theta N^{\delta - \delta_0}. \tag{14}$$

It follows that the number of roots of function f(b) = 0 is completely determined by the discriminant \triangle (see Fig. 15):

- If $\triangle < 0$, the function f(b) = 0 has no root.



Fig. 15 A schematic diagram of the number of roots of function f(b) as Δ changes



– If $\triangle > 0$, the function f(b) = 0 has two positive roots

$$b_1^* = \frac{\Phi\alpha\theta - \gamma N^{\delta - \delta_0 - 1} - \sqrt{\Delta}}{2\gamma N^{\delta - \delta_0 - 1}}, \ b_2^* = \frac{\Phi\alpha\theta - \gamma N^{\delta - \delta_0 - 1} + \sqrt{\Delta}}{2\gamma N^{\delta - \delta_0 - 1}} < b_0, \ (15)$$

since
$$b_1^*b_2^*=\frac{\alpha^2N^{\delta_0+2-\delta}\Phi\theta}{\gamma}>0$$
 and $b_1^*+b_2^*=\frac{\Phi\alpha\theta N^{\delta_0+1-\delta}}{\gamma}-1>0$.

Therefore, we can conclude that:

- Assume that $\Delta < 0$, then we have $\lambda_1(\hat{E}^*) + \lambda_2(\hat{E}^*) < 0$, i.e., \hat{E}^* is locally asymptotically stable.
- Assume that $\Delta > 0$. If $b < b_1^*$ or $b_0 > b > b_2^*$, we have $\lambda_1(\hat{E}^*) + \lambda_2(\hat{E}^*) < 0$, i.e., \hat{E}^* is locally asymptotically stable, while if $b_1^* < b < b_2^*$, we have $\lambda_1(\hat{E}^*) + \lambda_2(\hat{E}^*) > 0$, i.e., \hat{E}^* is unstable. It follows that two Hopf bifurcations occur at $b = b_1^*$ and $b = b_2^*$, respectively.

Since $\Phi > \frac{\gamma(1+b)N^{\delta-\delta_0-1}}{\alpha\theta} \Leftrightarrow N^{\delta_0+1-\delta} < \frac{\Phi\alpha\theta}{\gamma(1+b)}$, the system has an equilibrium \hat{E}^* if $N^{\delta_0+1-\delta} < \frac{\Phi\alpha\theta}{\gamma(1+b)}$. In the following, we choose N to be the bifurcation parameter. By (13) we have

$$f(N) = b(1+b)\gamma N^{\delta-\delta_0-1} + \alpha^2 \Phi \theta N - \alpha b \Phi \theta$$

and

$$f'(N) = (\delta - \delta_0 - 1)b(1+b)\gamma N^{\delta - \delta_0 - 2} + \alpha^2 \Phi \theta.$$

It follows that

– When $\delta > \delta_0 + 1$, the system has an equilibrium \hat{E}^* if

$$N < \frac{\Phi\alpha\theta}{\gamma(1+b)}^{\frac{1}{\delta-\delta_0-1}} := N_0.$$

In this case, we have f(0) < 0, $f(N_0) > 0$ and f'(N) > 0, which indicates that f(N) = 0 has a unique positive root $N^* \in (0, N_0)$. Therefore, \hat{E}^* is unstable



42 Page 46 of 53 T. Feng et al.

if $N \in (0, N^*)$; while it is locally asymptotically stable if $N \in (N^*, N_0)$. By a standard argument (Qiu and Zhu 2016), a Hopf bifurcation occurs at $N = N^*$.

- When $\delta < \delta_0 + 1$, \hat{E}^* exists if $N > N_0$. In this case, if

$$N < \frac{\alpha^2 \Phi \theta}{(1 + \delta_0 - \delta)b(1 + b)\gamma} \xrightarrow{\frac{1}{\delta - \delta_0 - 2}} := N_1,$$

we have f'(N) < 0, while if $N > N_1$ we have f'(N) > 0. Since f(0) > 0 and $f(N_0) > 0$, we have the following results: (a) if $N_0 > N_1$, we have f(N) > 0 for any $N \in (N_0, \infty)$, which indicates that \hat{E}^* is locally asymptotically stable; (b) if $N_0 < N_1$ and $f(N_1) > 0$, we have $f(N) > f(N_1) > 0$ for any $N \in (N_0, \infty)$, which indicates that \hat{E}^* is locally asymptotically stable; (c) if $N_0 < N_1$ and $f(N_1) < 0$, we know that f(N) = 0 has two roots N_1^*, N_2^* , where $N_0 < N_1^* < N_1 < N_2^*$. It follows that f(N) > 0 if $N \in (N_0, N_1^*) \bigcup (N_2^*, \infty)$, and f(N) < 0 if $N \in (N_1^*, N_2^*)$, which indicates that \hat{E}^* is locally asymptotically stable if $N \in (N_0, N_1^*) \bigcup (N_2^*, \infty)$, which indicates that \hat{E}^* is locally asymptotically stable if $N \in (N_0, N_1^*) \bigcup (N_2^*, \infty)$, while it is unstable if $N \in (N_1^*, N_2^*)$. By a standard argument (Qiu and Zhu 2016), two Hopf bifurcations occur at $N = N_1^*$ and $N = N_2^*$, respectively.

Model IV The System (10) always has two equilibria E_0^* , E_1^* . The Jacobian matrix of the System (10) evaluated at E_0^* is

$$J|_{(E_0^*)} = \begin{pmatrix} \frac{KN^{\delta-\delta_0}}{\sigma\theta} - 1 & 0 \\ -\alpha KN^{\delta+1} & -\frac{\gamma}{K} \end{pmatrix}.$$

Direct computation yields

$$\lambda_1(E_0^*) = -\frac{\gamma}{K} < 0, \text{ and } \lambda_2(E_0^*) = \frac{KN^{\delta - \delta_0}}{\varPhi\theta} - 1,$$

which indicates that the equilibrium E_0^* is locally asymptotically stable if $\lambda_2(E_0^*) < 0 \Leftrightarrow \Phi > \frac{KN^{\delta-\delta_0}}{\theta}$, and it is unstable if $\Phi < \frac{KN^{\delta-\delta_0}}{\theta}$. Similarly, we can obtain that E_1^* is locally asymptotically stable if $\Phi < \frac{KN^{\delta-\delta_0}}{\theta} \frac{\gamma}{\gamma + \alpha KN}$, and it is unstable if $\Phi > \frac{KN^{\delta-\delta_0}}{\theta} \frac{\gamma}{\gamma + \alpha KN}$.

Case (1) $\Phi > \frac{KN^{\delta-\delta_0}}{\theta}$. In this case, the System (10) has no interior equilibrium with two equilibria on the boundary Ω : E_0^* being locally asymptotically stable and E_1^* being unstable. It follows from the Pioncare-Bendixson theorem (Hale 1980) that all solutions of System (10) expect E_1^* converge to the equilibrium E_0^* , which indicates that E_0^* is globally asymptotically stable.

that E_0^* is globally asymptotically stable. Case (2) $\Phi < \frac{KN^{\delta-\delta_0}}{\theta} \frac{\gamma}{\gamma + \alpha KN}$. In this case, the System (10) has no interior equilibrium with two equilibria on the boundary Ω : E_0^* being unstable and E_1^* being locally asymptotically stable. It follows from the Pioncare-Bendixson theorem (Hale 1980)



that all solutions of System (10) expect E_0^* converge to the equilibrium E_1^* , which indicates that E_1^* is globally asymptotically stable.

Case (3) $\frac{KN^{\delta-\delta_0}}{\theta} \frac{\gamma}{\gamma + \alpha KN} < \Phi < \frac{KN^{\delta-\delta_0}}{\theta}$. In this case, the System (10) admits a unique interior equilibrium \hat{E}^* . The Jacobian matrix of the System (10) evaluated at \hat{E}^* is

$$J|_{(\hat{E}^*)} = \begin{pmatrix} 0 & \frac{\hat{x}^*(1-\hat{x}^*)}{\hat{D}^*} \\ -\alpha N \hat{D}^* - \frac{\gamma}{K} - \alpha N \hat{x}^* \end{pmatrix}.$$

Direct computation yields

$$\lambda_1(\hat{E}^*) + \lambda_2(\hat{E}^*) = -\left(\frac{\gamma}{K} + \alpha N \hat{x}^*\right) < 0$$

and

$$\lambda_1(\hat{E}^*)\lambda_2(\hat{E}^*) = \alpha N\hat{x}^*(1-\hat{x}^*) > 0.$$

It follows that $\lambda_1(\hat{E}^*) < 0$, $\lambda_2(\hat{E}^*) < 0$, i.e., \hat{E}^* is locally asymptotically stable. To show the globally asymptotically stable of \hat{E}^* , we only need to rule out the existence of periodic orbit for the System (10). Assume that $\Gamma(t) = (x(t), D(t))$ is an arbitrary nontrivial periodic orbit of the System (10) with the least period T > 0, and J(x(t), D(t)) is the Jacobian matrix of System (10) around the periodic solution (x(t), D(t)). Let

$$\begin{split} \Delta(\varGamma(t)) &:= \int_0^T \operatorname{Trac}(J(x(t),D(t))) dt \\ &= \int_0^T \left(\frac{D(t)\theta \Phi N^{\delta_0}}{\left[D(t)x(t) + \Phi \theta N^{\delta_0}(1-x(t))\right]^2} - 1 - \frac{\gamma}{K} - \alpha N x(t) \right) dt. \end{split}$$

Since

$$x' = x \left\lceil \frac{D}{Dx + \Phi \theta N^{\delta_0} (1 - x)} - 1 \right\rceil,$$

we have

$$\frac{D\Phi N^{\delta_0}}{\left[Dx + \Phi\theta N^{\delta_0}(1-x)\right]^2} = \left(\frac{x'}{x} + 1\right)^2 \frac{\theta\Phi N^{\delta_0}}{D}$$
$$= \frac{x'}{x} + 1 - \frac{{x'}^2}{x(1-x)} - \frac{x'}{1-x}.$$



42 Page 48 of 53 T. Feng et al.

It follows that

$$\begin{split} \Delta(\Gamma(t)) &= \int_0^T \left(\frac{x'(t)}{x(t)} - \frac{x'(t)^2}{x(t)(1 - x(t))} - \frac{x'(t)}{1 - x(t)} - \frac{\gamma}{K} - \alpha N x(t) \right) dt \\ &= \int_0^T \left(\frac{x'(t)}{x(t)} - \frac{x'(t)}{1 - x(t)} \right) dt \\ &+ \int_0^T \left(-\frac{x'(t)^2}{x(t)(1 - x(t))} - \frac{\gamma}{K} - \alpha N x(t) \right) dt \\ &< 0. \end{split}$$

By the divergency criterion (Hale 1980), all the periodic solutions must be orbitally stable. This contradicts the local stability of the equilibrium \hat{E}^* . Therefore, the equilibrium \hat{E}^* is globally asymptotically stable.

Declarations

Conflict of interest The authors declare that they have no conflict of interest.

References

- Allen LJS, Lahodny GE Jr (2012) Extinction thresholds in deterministic and stochastic epidemic models. J Biol Dyn 6(2):590–611
- Arcuri A, Lanchier N (2017) Stochastic spatial model for the division of labor in social insects. Math Models Methods Appl Sci 27(01):45–73
- Banks H, Banks J, Bommarco R, Laubmeier A, Myers N, Rundlöf M, Tillman K (2017) Modeling bumble bee population dynamics with delay differential equations. Ecol Model 351:14–23
- Barton BT, Hodge ME, Speights CJ, Autrey AM, Lashley MA, Klink VP (2018) Testing the AC/DC hypothesis: rock and roll is noise pollution and weakens a trophic cascade. Ecol Evol 8(15):7649–7656
- Beckers R, Goss S, Deneubourg JL, Pasteels JM (1989) Colony size, communication and ant foraging strategy. Psyche A J Entomol 96(3–4):239–256
- Benaïm M, Schreiber SJ (2019) Persistence and extinction for stochastic ecological models with internal and external variables. J Math Biol 79(1):393–431
- Blanchard GB, Orledge GM, Reynolds SE, Franks NR (2000) Division of labour and seasonality in the ant Leptothorax albipennis: worker corpulence and its influence on behaviour. Anim Behav 59(4):723–738
- Bonabeau E, obkowski A, Theraulaz G, Deneubourg J-L (1997) Adaptive task allocation inspired by a model of division of labor in social insects. In: Biocomputing and emergent computation: proceedings of BCEC97. World Scientific Press, pp 36–45. https://doi.org/10.5555/648178.751316
- Bourke AFG (1999) Colony size, social complexity and reproductive conflict in social insects. J Evolut Biol 12:245–257
- Britton T (2010) Stochastic epidemic models: a survey. Math Biosci 225(1):24-35
- Cai Y, Kang Y, Banerjee M, Wang W (2015) A stochastic SIRS epidemic model with infectious force under intervention strategies. J Differ Equ 259(12):7463–7502
- Cai Y, Kang Y, Wang W (2017) A stochastic SIRS epidemic model with nonlinear incidence rate. Appl Math Comput 305(20):221–240
- Cai Y, Li J, Kang Y, Wang K, Wang W (2020) The fluctuation impact of human mobility on the influenza transmission. J Franklin Inst 357(13):8899–8924
- Cammaerts MC, Cammaerts D (2018) Impact of environmental noise on insects physiology and ethology-a study on ants as models. Biol Eng Med 3:1–8



- Charbonneau D, Dornhaus A (2015a) When doing nothing is something. How task allocation strategies compromise between flexibility, efficiency, and inactive agents. J Bioecon 17(3):217–242
- Charbonneau D, Dornhaus A (2015b) Workers 'specialized' on inactivity: behavioral consistency of inactive workers and their role in task allocation. Behav Ecol Sociobiol 69(9):1459–1472
- Charbonneau D, Hillis N, Dornhaus A (2015) 'lazy' in nature: ant colony time budgets show high inactivity in the field as well as in the lab. Insectes Sociaux 62(1):31–35
- Charbonneau D, Poff C, Nguyen H, Shin MC, Kierstead K, Dornhaus A (2017) Who are the "lazy" ants? The function of inactivity in social insects and a possible role of constraint: inactive ants are corpulent and may be young and/or selfish. Integr Comp Biol 57(3):649–667
- Charbonneau D, Sasaki T, Dornhaus A (2017b) Who needs lazyworkers? Inactive workers act as a reservelabor force replacing active workers, but inactive workers are not replaced when they are removed. PloS One 12(9):e0184074
- Chen J, Messan K, Messan MR, DeGrandi-Hoffman G, Bai D, Kang Y (2020) How to model honeybee population dynamics: stage structure and seasonality. Math Appl Sci Eng 1(2):91–206
- Chown SL, Marais E, Terblanche JS, Klok CJ, Lighton JRB, Blackburn TM (2007) Scaling of insect metabolic rate is inconsistent with the nutrient supply network model. Funct Ecol 21(2):282–290
- Cole BJ (1986) The social behavior of Leptothorax allardycei (Hymenoptera, Formicidae): time budgets and the evolution of worker reproduction. Behav Ecol Sociobiol 18(3):165–173
- Corbara B, Lachaud JP, Fresneau D (1989) Individual variability, social structure and division of labour in the ponerine ant ectatomma ruidum Roger (Hymenoptera, Formicidae). Ethology 82(2):89–100
- Cornejo A, Dornhaus A, Lynch N, Nagpal R (2014) Task allocation in ant colonies. In: Kuhn F (ed) Distributed computing. DISC 2014. Lecture Notes in Computer Science, vol 8784. Springer, Berlin, Heidelberg. https://doi.org/10.1007/978-3-662-45174-8_4
- Costello RA, Symes LB (2014) Effects of anthropogenic noise on male signalling behaviour and female phonotaxis in Oecanthus tree crickets. Anim Behav 95:15–22
- Couzin ID, Franks NR (2003) Self-organized lane formation and optimized traffic flow in army ants. Proc R Soc Lond Ser B Biol Sci 270(1511):139–146
- DeLillo D (1999) White noise. Penguin, London
- Dornhaus A (2008) Specialization does not predict individual efficiency in an ant. PLoS Biol 6(11):2368–2375
- Dornhaus A, Holley JA, Pook VG, Worswick G, Franks NR (2008) Why do not all workers work? Colony size and workload during emigrations in the ant Temnothorax albipennis. Behav Ecol Sociobiol 63(1):43–51
- Dornhaus A, Powell S, Bengston S (2012) Group size and its effects on collective organization. Annu Rev Entomol 57:123–141
- Dussutour A, Beekman M, Nicolis SC, Meyer B (2009) Noise improves collective decision-making by ants in dynamic environments. Proc R Soc B Biol Sci 276(1677):4353–4361
- Evans SN, Ralph PL, Schreiber SJ, Sen A (2013) Stochastic population growth in spatially heterogeneous environments. J Math Biol 66(3):423–476
- Feinerman O, Korman A (2017) Individual versus collective cognition in social insects. J Exp Biol 220(1):73–82
- Fellers JH (1989) Daily and seasonal activity in woodland ants. Oecologia 78(1):69-76
- Feng T, Qiu Z, Meng X (2019) Dynamics of a stochastic hepatitis c virus system with host immunity. Discrete Contin Dyn Syst B 24(12):6367–6385
- Fewell JH, Harrison JF (2016) Scaling of work and energy use in social insect colonies. Behav Ecol Sociobiol 70(7):1047–1061
- Fewell JH, Winston ML (1992) Colony state and regulation of pollen foraging in the honey bee, Apis mellifera L. Behav Ecol Sociobiol 30(6):387–393
- Fjerdingstad EJ, Crozier RH (2006) The evolution of worker caste diversity in social insects. Am Nat 167(3):390-400
- Franks NR, Dornhaus A, Best CS, Jones EL (2006) Decision making by small and large house-hunting ant colonies: one size fits all. Anim Behav 72(3):611–616
- Franks NR, Partridge LW (1993) Lanchester battles and the evolution of combat in ants. Anim Behav 45(1):197–199
- Fresneau D (1984) Développement ovarien et statut social chez une fourmi primitive Neoponera obscuricornis Emery (Hym. Formicidae, Ponerinae). Insectes Sociaux 31(4):387–402



42 Page 50 of 53 T. Feng et al.

Gadagkar R, Joshi N (1984) Social organisation in the Indian wasp ropalidia cyathiformis (Fab.)(hymenoptera: vespidae). Zeitschrift Für Tierpsychologie 64(1):15–32

Gardner KE, Foster RL, ODonnell S (2007) Experimental analysis of worker division of labor in bumblebee nest thermoregulation (Bombus huntii, Hymenoptera: Apidae). Behav Ecol Sociobiol 61(5):783–792

Glazier DS (2010) A unifying explanation for diverse metabolic scaling in animals and plants. Biol Rev 85(1):111–138

Gordon DM (1996) The organization of work in social insect colonies. Nature 380(6570):121-124

Gray A, Greenhalgh D, Hu L, Mao X, Pan J (2011) A stochastic differential equation sis epidemic model. SIAM J Appl Math 71(3):876–902

Guo X, Chen J, Azizi A, Fewell J, Kang Y (2020) Dynamics of social interactions, in the flow of information and disease spreading in social insects colonies: effects of environmental events and spatial heterogeneity. J Theor Biol. https://doi.org/10.1016/j.jtbi.2020.110191

Hale JK (1980) Ordinary differential equations. Krieger Publishing Company, Malabar

Hasegawa E, Ishii Y, Tada K, Kobayashi K, Yoshimura J (2016) Lazy workers are necessary for long-term sustainability in insect societies. Sci Rep 6(1):1–9

Hening A, Nguyen DH, Yin G (2018) Stochastic population growth in spatially heterogeneous environments: the density-dependent case. J Math Biol 76(3):697–754

Herbers JM (1983) Social organization in Leptothorax ants: within-and between-species patterns. Psyche A J Entomol 90(4):361–386

Herbers JM, Cunningham M (1983) Social organization in Leptothorax Longispinosus Mayr. Anim Behav 31(3):759–771

Higham DJ (2001) An algorithmic introduction to numerical simulation of stochastic differential equations. SIAM Rev 43(3):525–546

Holbrook CT, Barden PM, Fewell JH (2011) Division of labor increases with colony size in the harvester ant Pogonomyrmex californicus. Behav Ecol 22(5):960–966

Holbrook CT, Eriksson T, Overson R, Gadau J, Fewell JH (2013) Colony-size effects on task organization in the harvester ant Pogonomyrmex californicus. Insectes Sociaux 60(2):191–201

Hölldobler B, Wilson EO (1990) The ants. Belknap Press of Harvard University Press, Cambridge

Hölldobler B, Wilson EO (2009) The superorganism: the beauty, elegance, and strangeness of insect societies. WW Norton & Company, New York

Hou C, Kaspari M, Vander Zanden HB, Gillooly JF (2010) Energetic basis of colonial living in social insects. Proc Natl Acad Sci 107(8):3634–3638

Houston A, Schmid-Hempel P, Kacelnik A (1988) Foraging strategy, worker mortality, and the growth of the colony in social insects. Am Nat 131(1):107–114

Jandt JM, Robins N, Moore R, Dornhaus A (2012) Individual bumblebees vary in response to disturbance: a test of the defensive reserve hypothesis. Insectes Sociaux 59(3):313–321

Jeanne RL (2003) Social complexity in the Hymenoptera, with special attention to wasps. Kitkuchi T, Azuma N, Higashi S (eds) Genes, behaviors and evolution of social insects. Hokkaido University Press, Sapporo, Japan, pp 81–131

Jeanson R, Fewell JH, Gorelick R, Bertram SM (2007) Emergence of increased division of labor as a function of group size. Behav Ecol Sociobiol 62(2):289–298

Johnson BR (2002) Reallocation of labor in honeybee colonies during heat stress: the relative roles of task switching and the activation of reserve labor. Behav Ecol Sociobiol 51(2):188–196

Kang Y, Fewell JH (2015) Co-evolutionary dynamics of a social parasite-host interaction model: obligate versus facultative social parasitism. Nat Resour Model 28(4):398–455

Kang Y, Rodriguez-Rodriguez M, Evilsizor S (2015) Ecological and evolutionary dynamics of two-stage models of social insects with egg cannibalism. J Math Anal Appl 430(1):324–353

Kang Y, Theraulaz G (2016) Dynamical models of task organization in social insect colonies. Bull Math Biol 78(5):879–915

Kleiber M (1947) Body size and metabolic rate. Physiol Rev 27(4):511–541

Kleiber M et al (1932) Body size and metabolism. Hilgardia 6(11):315–353

Klein BA (2003) Signatures of sleep in a paper wasp. Sleep 26:A115-A116

Klein BA, Klein A, Wray MK, Mueller UG, Seeley TD (2010) Sleep deprivation impairs precision of waggle dance signaling in honey bees. Proc Natl Acad Sci 107(52):22705–22709

Klein BA, Seeley TD (2011) Work or sleep? Honeybee foragers opportunistically nap during the day when forage is not available. Anim Behav 82(1):77–83



- Kwapich CL, Tschinkel WR (2013) Demography, demand, death, and the seasonal allocation of labor in the Florida harvester ant (Pogonomyrmex badius). Behav Ecol Sociobiol 67(12):2011–2027
- Lee Y, Kim H, Kang TJ, Jang Y (2012) Stress response to acoustic stimuli in an aphid: a behavioral bioassay model. Entomol Res 42(6):320–329
- Lighton JR, Bartholomew GA, Feener DH (1987) Energetics of locomotion and load carriage and a model of the energy cost of foraging in the leaf-cutting ant Atta Colombica Guer. Physiological Zoology 60(5):524–537
- Lindauer M (1952) Ein beitrag zur frage der arbeitsteilung im bienenstaat. Zeitschrift Für Vergleichende Physiologie 34(4):299–345
- Liu M, Liz E, Röst G (2015) Endemic bubbles generated by delayed behavioral response: global stability and bifurcation switches in an sis model. SIAM J Appl Math 75(1):75–91
- Magal P, Webb G, Wu Y (2019) An environmental model of honey bee colony collapse due to pesticide contamination. Bull Math Biol 81(12):4908–4931
- Mailleux AC, Deneubourg JL, Detrain C (2003) How does colony growth influence communication in ants? Insectes Sociaux 50(1):24–31
- Maistrello L, Sbrenna G (1999) Behavioural differences between male and female replacement reproductives in Kalotermes flavicollis (isoptera, Kalotermitidae). Insectes Sociaux 46(2):186–191
- Messan K, Messan MR, Chen J, DeGrandi-Hoffman G, Kang Y (2020) Population dynamics of varroa mite and honeybee: effects of parasitism with age structure and seasonality. arXiv preprint arXiv:2003.12089
- Messan MR, Page RE Jr, Kang Y (2018) Effects of vitellogenin in age polyethism and population dynamics of honeybees. Ecol Model 388:88–107
- Moore D, Angel JE, Cheeseman IM, Fahrbach SE, Robinson GE (1998) Timekeeping in the honey bee colony: integration of circadian rhythms and division of labor. Behav Ecol Sociobiol 43(3):147–160
- Muscedere ML, Willey TA, Traniello JF (2009) Age and task efficiency in the ant Pheidole dentata: young minor workers are not specialist nurses. Anim Behav 77(4):911–918
- Myerscough M, Oldroyd B (2004) Simulation models of the role of genetic variability in social insect task allocation. Insectes Sociaux 51(2):146–152
- Naug D (2009) Structure and resilience of the social network in an insect colony as a function of colony size. Behav Ecol Sociobiol 63(7):1023–1028
- O'Donnell S (1998) Effects of experimental forager removals on division of labour in the primitively eusocial wasp Polistes instabilis (Hymenoptera: Vespidae). Behaviour 135(2):173–193
- Oster GF, Wilson EO (1978) Caste and ecology in the social insects. Princeton University Press, Princeton Ovaskainen O, Meerson B (2010) Stochastic models of population extinction. Trends Ecol Evol 25(11):643–652
- Pol R, de Casenave JL (2004) Activity patterns of harvester ants Pogonomyrmex pronotalis and Pogonomyrmex rastratus in the central Monte desert, Argentina. J Insect Behav 17(5):647–661
- Qiu Z, Zhu H (2016) Complex dynamics of a nutrient-plankton system with nonlinear phytoplankton mortality and allelopathy. Discrete Contin Dyn Syst B 21(8):2703–2728
- Ramsch K, Reid CR, Beekman M, Middendorf M (2012) A mathematical model of foraging in a dynamic environment by trail-laying argentine ants. J Theor Biol 306:32–45
- Ranjan A, Raghavan N, Shubhakar K, Thamankar R, Molina J, O'Shea S, Bosman M, Pey K (2016) CAFM based spectroscopy of stress-induced defects in HFO 2 with experimental evidence of the clustering model and metastable vacancy defect state. In: 2016 IEEE International Reliability Physics Symposium (IRPS). IEEE , pp. 7A–4
- Retana J, Cerdá X (1990) Social Organization of Cataglyphis cursor ant colonies (Hymenoptera, Formicidae): inter-, and intraspecific Comparisons. Ethology 84(2):105–122
- Retana J, Cerda X (1991) Behavioural variability and development of Cataglyphis cursor ant workers (Hymenoptera, Formicidae) 1. Ethology 89(4):275–286
- Robinson EJ, Feinerman O, Franks NR (2009) Flexible task allocation and the organization of work in ants. Proc R Soc B Biol Sci 276(1677):4373–4380
- Rodriguez MR, Smith N, Phan T, Woodbury J, Kang Y (2018) Interactions between leaf-cutter ants and fungus garden: effects of division of labor, age polyethism, and egg cannibalism. Math Model Nat Phenom 13(3):30
- Rodriguez-Rodriguez M, Kang Y (2016) Colony and evolutionary dynamics of a two-stage model with brood cannibalism and division of labor in social insects. Nat Resour Model 29(4):633–662



42 Page 52 of 53 T. Feng et al.

Ruel C, Cerda X, Boulay R (2012) Behaviour-mediated group size effect constrains reproductive decisions in a social insect. Anim Behav 84(4):853–860

Saffman P, Delbrück M (1975) Brownian motion in biological membranes. Proc Natl Acad Sci 72(8):3111–3113

Schmid-Hempel P (1990) Reproductive competition and the evolution of work load in social insects. Am Nat 135(4):501–526

Shik JZ (2010) The metabolic costs of building ant colonies from variably sized subunits. Behav Ecol Sociobiol 64(12):1981–1990

Slatkin M (1978) The dynamics of a population in a Markovian environment. Ecology 59(2):249-256

Spagnolo B, Valenti D, Fiasconaro A (2004) A Noise in ecosystems: a short review. Math Biosci Eng 1(1):185-211

Sumpter D, Pratt S (2003) A modelling framework for understanding social insect foraging. Behav Ecol Sociobiol 53(3):131–144

Theraulaz G, Bonabeau E, Denuebourg J (1998) Response threshold reinforcements and division of labour in insect societies. Proc R Soc Lond Ser B Biol Sci 265(1393):327–332

Thieme HR (2003) Mathematics in population biology. Princeton University Press, Princeton

Thomas M, Framenau V (2005) Foraging decisions of individual workers vary with colony size in the greenhead ant Rhytidoponera metallica (Formicidae, Ectatomminae). Insectes Sociaux 52(1):26–30

Tietjen WJ (1986) Effects of colony size on web structure and behavior of the social spider Mallos gregalis (Araneae, Dictynidae). J Arachnol 14:145–157

Tschinkel WR (1993) Sociometry and sociogenesis of colonies of the fire ant solenopsis invicta during one annual cycle: ecological archives M063–002. Ecol Monogr 63(4):425–457

Tschinkel WR, Adams ES, Macom T (1995) Territory area and colony size in the fire ant Solenopsis invicta. J Anim Ecol 64:473–480

Udiani O, Pinter-Wollman N, Kang Y (2015) Identifying robustness in the regulation of collective foraging of ant colonies using an interaction-based model with backward bifurcation. J Teor Biol 367:61–75

Waters JS (2014) Theoretical and empirical perspectives on the scaling of supply and demand in social insect colonies. Entomol Exp Appl 150(2):99–112

Waters JS, Holbrook CT, Fewell JH, Harrison JF (2010) Allometric scaling of metabolism, growth, and activity in whole colonies of the seed-harvester ant Pogonomyrmex californicus. Am Nat 176(4):501–510

Wilson EO (1971) The insect societies. Harvard University Press, Cambridge

Wu F, Xu Y (2009) Stochastic Lotka-Volterra population dynamics with infinite delay. SIAM J Appl Math 70(3):641–657

Publisher's Note Springer Nature remains neutral with regard to jurisdictional claims in published maps and institutional affiliations.

Affiliations

Tao Feng^{1,2} · Daniel Charbonneau³ · Zhipeng Qiu¹ · Yun Kang²

✓ Yun Kang yun.kang@asu.edu

> Tao Feng tfeng.math@gmail.com

Daniel Charbonneau

charbonneau.daniel@gmail.com

Zhipeng Qiu nustqzp@njust.edu.cn

Department of Mathematics, Nanjing University of Science and Technology, Nanjing 210094, People's Republic of China



- Sciences and Mathematics Faculty, College of Integrative Sciences and Arts, Arizona State University, Mesa, AZ 85212, USA
- School of Life Sciences, Arizona State University, Tempe, AZ 85287, USA

